Development and Experimental Study of Machining Parameters in Ultrasonic Vibration-assisted Turning

BIKASH CHANDRA BEHERA

Department of Mechanical Engineering

National Institute of Technology, Rourkela-769008, India

2011

Development and Experimental Study of Machining Parameters in Ultrasonic Vibration-assisted Turning

Thesis submitted in partial fulfillment of

the requirements for the degree of

Master of Technology (Research)

In

Mechanical engineering

By

Bikash Chandra Behera

Roll No: 609ME602

Under the guidance of

Prof S. K. Sahoo

Prof K.P. Maity

Department of Mechanical Engineering

National Institute of Technology, Rourkela-769008, India

2011

Department of Mechanical Engineering

National Institute of Technology, Rourkela

Rourkela 769008, Orissa, India

CERTIFICATE

This is to certify that the thesis entitled, **"Development and Experimental Study of Machining Parameters in Ultrasonic Vibration-assisted Turning"** *submitted by* ***Mr. Bikash Chandra Behera*** *in partial fulfillment of requirements for the award of Degree of Master of Technology (Research) in* ***Mechanical Engineering*** *at National Institute of Technology, Rourkela is an authentic work carried out by him under our guidance and supervision. To the best of our knowledge the matter embodied in the thesis has not been submitted to any other University or Institute for the award of any Degree or Diploma.*

Prof S.K. Sahoo
Department of Mechanical Engineering
NIT Rourkela

Prof K.P. Maity
Department of Mechanical Engineering
NIT Rourkela

ACKNOWLEDGEMENT

I take this opportunity to express my reverence to my supervisor Prof. S.K. Sahoo and Co-supervisor Prof. K.P. Maity for their guidance, inspiration and innovative technical discussions during the course of this work. Their perpetual energy and enthusiasm in research had motivated others, including me. In addition, they were always accessible and willing to help their students with their research. As a result, research life became smooth and rewarding for me.

Prof.C.K.Biswas, Prof K.C. Biswal, Prof S.C.Mishra and Prof. R.K.Sahoo deserves special thanks as my thesis committee members and Chairman for their critical suggestions.

I also express my sincere gratitude to all faculty and staffs members of Mechanical Engineering Department and Central workshop for providing valuable departmental facilities.

I would like to express my thanks to Mr. L.N.Patra, Mr. B. N. Sahoo, Mr M.P. Rout and Mr. K.K. Kanaujia for helping me for conducting experimental works.

I would like to thank all my friends and especially my classmates for all the thoughtful and mind stimulating discussions we had, which prompted us to think beyond the obvious.

Last but not least I would like to thank my parents, who taught me the value of hard work by their own example. They rendered me enormous support being apart during the whole tenure of my stay in NIT Rourkela.

Bikash Chandra Behera
Roll No: 609ME602

ABSTRACT

In recent years applications of hard materials in different industries, like aerospace, defence and petrochemicals sectors etc. have been increased remarkably. The machining of these hard materials is very difficult in conventional turning process. Ultrasonic assisted turning is a suitable and advanced process for machining hard and brittle material because of its intermittent cutting mechanism. In the present work, an ultrasonic vibratory tool (UVT) is designed and analyzed using ANSYS® environment for calculation of its natural frequency and working amplitude of vibration. An ultrasonic assisted turning system is designed considering cutting tool as a cantilever beam. Experimental study has been carried out to find the difference between ultrasonic-assisted and conventional turning at different cutting conditions taking carbon steel (a general purpose engineering material) as the work piece material. It is found that ultrasonic assisted turning reduces the surface roughness and cutting force in comparison with conventional turning. It is well known that cutting force and surface finish/roughness are two major parameters which affect the productivity of the turning process. In the present work, Grey based Taguchi method is used to optimize both cutting force and surface roughness to find the best possible machining parameters under the used experimental working conditions. Also, second order response models for the surface roughness and cutting force are developed and confirmation experiments are conducted.

Key words: UAT, UVT, Longitudinal vibration, Modal analysis, Harmonic analysis, Triangular rule, GRA, RSM

ABBREVIATIONS

ANOVA	Analysis of variance
ANSYS	Analysis of system
CNC	Computer numerical control
CT	Conventional turning
1D	One-dimensional
2D	Two-dimensional
3D	Three dimensional
DAQ	Data acquisitions
DF	Degree of freedom
DOE	Design of experiment
FEM	Finite element modeling
FRF	Frequency response function
GRA	Grey relation analysis
GRG	Grey relation grade
Hz	Hertz
MB	Mega byte
MMC	Metal matrix composite
MS	Mean square
NC	Numerical control
NI	National instrument
PC	Personal computer
PZT	Piezoelectric transducer
RAM	Random access memory
RSM	Response surface methodology
SEM	Scanning electron microscope
SS	Sum of square
TWCR	Tool work-piece contact ratio
UAC	Ultrasonic assisted cutting
UAT	Ultrasonic assisted turning
UVT	Ultrasonic vibratory tool

NOMENCLATURE

A	Area of cross section
a	Amplitude
a_c	Acceleration
C	Velocity of sound
cos	Cosine
D	Diameter
d	Depth of cut
E	Young's modulus
F_m	Forces of momentum
F_x	Cutting force in X-axis direction
F_y	Cutting force in Y-axis direction
F_z	Cutting force in Z-axis direction
f	Frequency
h	Height
i	Complex number
K	Stress concentration
L	Length
M	Mass
M_z	Moment in Z-axis direction
N	Spindle speed
R_a	Surface roughness
r	Radius
S	Feed
sin	Sine
s	Stress
s_m	Maximum stress
t	Time
V	Cutting velocity
V_c	Velocity of chip
V_t	Velocity of tip
v	Velocity
W	Weight
x_n	Nodal plane
λ	Wave length
γ	Poison's ratio
γ_i	Grey relational grade
ξ	Displacement
ξ_M	Maximum displacement
Δ	Triangle
ρ	Density
ω	Angular velocity

LIST OF FIGURES

Page No.

CHAPTER 5

LIST OF TABLE

Page No.

CONTENTS

Chapter-1

Introduction

CHAPTER 1

INTRODUCTION

1.1 Outline of Ultrasonic Assisted Turning

Ultrasonic provides a group of facilities in our life, such as in manufacturing, medical, communications, transport, industries, etc. In the machining process, ultrasonic can bring about improvements when applied in the correct manner. Ultrasonic assisted turning is a cutting technique in which a certain frequency (in ultrasonic range) of vibration is applied to the cutting tool or the work-piece (besides the original relative motion between these two) to achieve better cutting performance (Shamoto et al. [1]). A number of experimental setup has been proposed to make the process simpler, but the tendency is to apply the process to a wide range of materials and to study the effect of machining parameters. Many researchers have reported significant improvements in noise reduction, tool wear reduction, surface finish, etc. by applying ultrasonic vibration during machining operations in general, the turning processes in particular [2,3], This pointed out possible advantages of the ultrasonic technology for industrial machining. The present research is particularly focused on ultrasonic vibration-assisted turning.

In ultrasonic assisted machining, vibration amplitude (normally sine wave) lead to an alternating gap during cutting and was identified as an important mechanism in vibration cutting. Increasing the vibration amplitude means an enlargement in the gap that allows more cutting fluid to extract the heat during the cutting process, thus enhancing the tool's life, improved work-piece finish, reduction in cutting forces and decreasing the chance of build-up-edge formation [4-6]. In turning process there are three independent principal directions in which ultrasonic vibration can be applied (Figure 1.1).Significant advantages were obtained when the usual continuous interaction between the cutting tip and the work-piece was replaced by intermittent cutting [7-8]. However, when the cutting tip is vibrated ultrasonically the following restrictions are imposed:

Tangential direction: $V_c=\pi ND < V_t=2\pi af$

Where V_c is the cutting speed during turning operation, N is the rotational speed of work-piece, V_t is the tip velocity, f is the frequency of vibration and a is the amplitude of vibration. A rheological model of ultrasonic vibration cutting projected by Astashev [7] and ensuing

experiments confirmed a evident reduction in the cutting force for ultrasonic cutting with vibration in tangential direction (f =20kHz, a=10μm). It was also reported that cutting force reduction was less at higher cutting speeds and, with a cutting speeds exceeding a certain level ($V_t > \omega a$, where ω is the angular frequency), vibration did not affect the cutting force. The resistance forces were considered to be caused by plastic deformation of the layer being cut off by frictional forces acting on the working faces of the cutting tool. These experimental results have been explained theoretically by Astashev and Babitsky [9] within the frame work of rheological models. Reduction in the cutting force caused by superimposition of ultrasonic vibration was derived for the elasto-plastic material model. It was concluded that the vibrating process transforms and reduces the friction force due to the effect of dynamic fluidization of dry friction. Dynamic characteristics of transformed machining processes were obtained, including the dependence of reduced cutting forces on the material and vibrations parameters. Dynamics of an ultrasonic cutting machine under technological load was investigated and the nonlinear amplitude response of vibrating tool in the process of cutting was obtained by many researchers. The auto resonant control system keeping the resonant conditions of excitation under variable technological loads was constructed by Astashev and Babitsky [9].

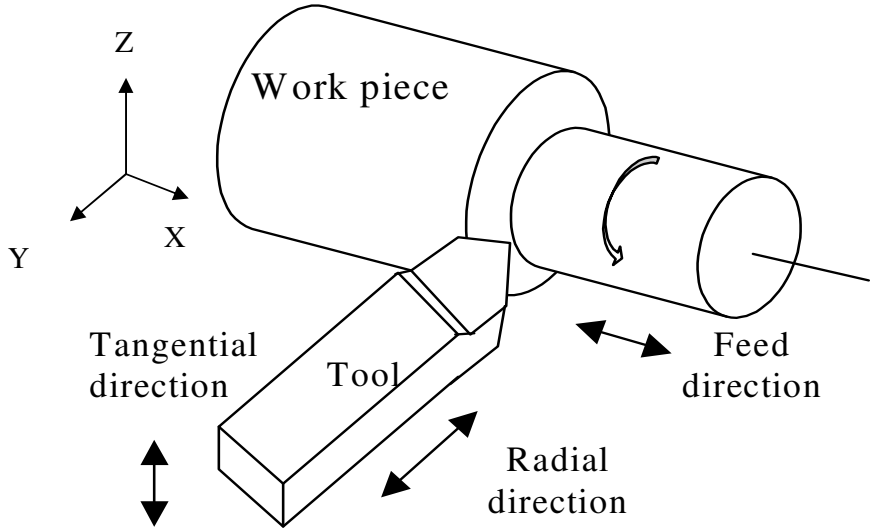

Figure1.1 Principal vibration directions during ultrasonically assisted turning [10]

Babitsky et al [10] designed an auto resonant ultrasonic assisted turning system, maintaining the constant level of vibration provided by the transducer and therefore improving the precision of ultrasonic machining. Vibration in the feed directions was also studied. It was

pointed out that application of ultrasonic vibration along the feed direction enables overcoming the restriction on the level of rotational speeds, which is of great importance for industrial UAT requiring high levels of productivity.

Mashiko and Murakawa [11] developed practical ultrasonic vibration cutting tool system and their investigation on tool wear and surface finish in ultrasonic and conventional turning and they found that chipping of the cutting edge can be effectively prevented and good surface finish obtained in ultrasonic assisted turning. Some other researcher [12-18] also investigated on vibration assisted turning and they found that ultrasonic assisted turning improves surface finish and reduces average cutting forces as compared to conventional turning in case of hard and brittle material.

1.2 The Current Needs in Industry

Generally the machining surface quality is usually measured by the surface roughness and physical mechanical properties of the surface layer. The surface quality has a great impact on wear resistance, fatigue strength of the product and fit precision of the part. Hard and brittle material has excellent mechanical properties at low and intermediate temperature. It plays an important part in recent years in aerospace, nuclear and petroleum industries. Hard materials are very difficult to machine because of a tendency of the maximum temperature of tool face existing at the tip of tool. Micro welding at the tool tip and chip interface takes place so as to lead to the built up edge formation which effect the surface quality of material. In ultrasonic assisted turning these effects are reduced due its vibro-impact cutting.

1.3 Aim and Objectives of the Research

1.3.1 Aim of the research

The present research aims to get a technical understanding of the ultrasonic assisted turning process against the principal cutting force and surface roughness generation. The research includes the design and FEM analysis of ultrasonic vibratory tool, design and development of an ultrasonic assisted vibration turning system, taking cutting tool as a cantilever beam. Turning carbon steel work-piece material (a general purpose engineering material) using both conventional and ultrasonic assisted turning and analyzing the results. Mathematical relations between responses and factors of ultrasonic assisted turning (UAT) are developed and the ultrasonic turning process parameters are optimized.

1.3.2 Objectives of the present research

- FEM analysis of ultrasonic vibratory tool (UVT).
- Design and manufacture of the experimental set-up.

- Experimental investigations using both conventional and ultrasonic assisted turning processes taking a general purpose engineering material (carbon steel) as work-piece.
- Comparison of both conventional and ultrasonic assisted turning based on experimental data.
- Mathematical modeling of process parameters using response surface methodology (RSM).
- Optimization of the process parameters using grey based Taguchi method.

Chapter-2

Literature Survey

CHAPTER 2

LITERATURE SURVEY

2.1 Introduction

Ultrasonic vibration has been harnessed with considerable benefits for a variety of manufacturing processes, for example, ultrasonic cleaning, ultrasonic grinding, ultrasonic welding and ultrasonic turning etc. The ultrasonic vibration method in which periodic or oscillating cycles are forced on the cutting tool or the work-piece, besides the original relative motion between these two, so as to get improvements in cutting performance. The fundamental feature of Ultrasonic Assisted Turning (UAT) is that the tool face is separated from the work-piece repeatedly (velocity of the tool is more than cutting velocity during half of an oscillating cycle). First attempt to employ the ultrasonic power is attempted by Russian [2, 12] as well as Japanese [3, 13] researchers.

Kumabe [3] in his monograph summarized some of research results up to the time of his publication and also presented the outcomes of his own experiments on the application of ultrasonic vibrations for various conventional material removal processes. Markov [2, 14] in his book "ultrasonic machining of intractable materials" described the use of ultrasonic vibration in turning of heat resistance alloys. He applied vibration in his experiments in the radial and tangential direction with the help of a magnetostrictive transducer. He emphasized that rigidity of the system comprising a machine tool, fitting, cutting tool and work-piece is important. If rigidity of this system is not enough, the tool life is shortened and the overall advantage of UAT may be small. He also suggested that the influence of ultrasonic vibration on the turning process could be explained by the thermal effects, which cause softening and micro-melting of the deformed material in the contact points with the cutting tip and affect the nature of frictional processes at the tool chip interface considerably.

Shampto [1], Moriwaki et al.[8] explored ultra precision diamond turning of glass and SU303Se-JIS stainless steel by applying ultrasonic vibration (f=40kH_Z, a=3µm) to a single crystal diamond tool in the direction of cutting velocity. They argued that an increase in vibration frequency reduced generation of vibration marks at the finished surface. These experiments were carried out on an ultra precision turning machine and a mirror like finish of the stainless steel with a surface roughness of 0.026µm was obtained. An increased tool life was reported due to a reduction in both crater and flank wear.

Other notable works include that of Kim and Lee [15], experiments on the cutting of carbon fiber reinforced plastics, Weber et al. [16], find effect of cutting speed on surface roughness in UAT, Kim and Choi [17], use of UAT on brittle optical plastic, Locke and Rubenism [18], use of synthetic singe crystal diamond tools in UAT for manufacture of ultra precision parts and many more. The foremost part of the present study is to construct a vibration assisted turning system, by which various investigations can be carried out to analyze the process, which is the critical and essential component of this research.

2.2 Review of Ultrasonic Assisted Cutting

Ultrasonic assisted cutting technique is becoming very challenging in many recent engineering developments, especially in relation to surface finish and tool wear and material removal rate. The very basic component of ultrasonic assisted cutting system is piezoelectric transducer and ultrasonic vibratory tool. For different applications different designs have been developed, such as, ultrasonic assisted turning, welding, milling, drilling, grinding. Ultrasonic assisted machining technology has been studied by many cited references. All of these studies analyze in different ways, concept, design and dynamics of setup, characteristics and finite element modeling and comparison of cutting forces during machining processes.

2.2.1 Experimental study on ultrasonic assisted turning

Skelton [19] studied using ultrasonic vibration in turning operation, using a magnetostrictive transducer. He applied vibration in vertical and horizontal directions on carbide tip cutting tool, found that cutting force components are less than with a static tool, particularly at low cutting speeds and also justified it due to a reduction in the mechanical strength of the workpiece material in the presence of ultrasonic vibration.

Masahiko and Murakawa [11] developed an ultrasonic vibration cutting tool device which is more rigid and stable than which was used previously [7] by them. They observed that the chipping of the cutting edge is reduced and a good surface finish obtained by both continuous and intermittent cutting modes when cutting hardened steels.

Babitsky et al. [10] developed an auto resonant ultrasonic vibration turning system for turning of some modern aviation material. They applied ultrasonic vibration in the feed direction and compared conventional and ultrasonic turning. They found that the application of ultrasonic vibration can improve the surface quality considerably, up to 25–50%.

Zhong and Lin [20, 21] developed an ultrasonic vibration device to investigate diamond turning of an aluminum-based metal matrix composite (MMC) reinforced with SiC particles. In their experiments ultrasonic vibration is applied to the cutting tool, small-size vibration

device (without using booster) was designed to mount a piezoelectric transducer and cutting is done by vertical CNC milling machine. They found that surface roughness of the MMC samples cut with ultrasonic vibrations is better than that of the MMC sample cut conventionally; and also cutting parameters, like, depth of cut and cutting speed also affect the surface finish significantly and they adopted theory of light depression phenomenon for measurement.

Liu et al. [22] have performed experimental study on distinctiveness of ultrasonic vibration-assisted cutting of tungsten carbide material using a CNC lathe with CBN tool inserts. In their experiments they found that the radial force is much larger than the tangential and axial force as their vibration was is in cutting depth direction. The SEM observations on the machined work-piece surfaces and chip formation indicated that the critical condition for ductile mode cutting of tungsten carbide was mainly the maximum undeformed chip thickness when the tool cutting edge radius was fixed, that is, the ductile mode cutting can be achieved when the maximum undeformed chip thickness was smaller than a critical value. Corresponding to the chip formation mode (ductile or brittle), three types of the machined work-piece surfaces were obtained: fracture-free surface, semi-fractured surface and fractured surface. It was also found that the cutting speed has no significant effect on the ductile chip formation mode.

Chen et al. [23] performed experimental study on turning W-Fe-Ni alloy by conventional turning and ultrasonically assisted turning. They found that in ultrasonic assisted turning, feed rate still has significant influence on surface roughness, next to important factors are vibration parameters, while the influence of depth of cut and cutting speed on surface roughness become less profound than others parameters. Comparing with CT, the surface roughness machined by UAT reduced by the range of 7.05%-30.06%. They observed that UAT can give smoother surface, but the residual stress is larger than that in CT. It confirms that the rake surface of the vibration cutter has an intense ironing effect on the work piece surface.

Hsu et al. [24] study on the machining characteristics of Inconel 718 by combining ultrasonic vibration with high-temperature-aided cutting. Experiment is done using Taguchi experimental design to clarify the influence of various machining parameters on the machining characteristics. They found that the percentage contributions of the cutting tool, feed rate, working temperature and depth of cut for surface roughness are 33.16, 25.00, 13.36 and 9.17, respectively and the percentage contributions of the cutting speed, feed rate, cutting tool and depth of cut for cutting force are 22.27, 16.88, 13.80 and 13.37, respectively and also

found that Ultrasonic-aided cutting improved the surface roughness by 9.10–51.61%, as well as decreasing cutting force by 32.34–24.47%. As a result, ultrasonic-aided cutting can enhance the cutting quality of Inconel 718.

Nath et al. [25] studied the mechanism of UVC and proposed that it is influenced by three important parameters, namely, vibration frequency, vibration amplitude and working cutting speed that determine the cutting force. On their theoretical study they established that tool work piece contact ratio (TWCR) (Figure 2.1) plays a key role in the UVC process where increase in both the tool vibration parameters (frequency and amplitude of cutting tool) and decrease in cutting speed reduce the TWCR, which in turn reduces both cutting force and tool wear, and improves surface quality and prolongs tool life. They have successfully implemented this theory by means of turning Inconel 718 work piece material, both conventionally and ultrasonically, and found that TWCR plays key role in UVC method.

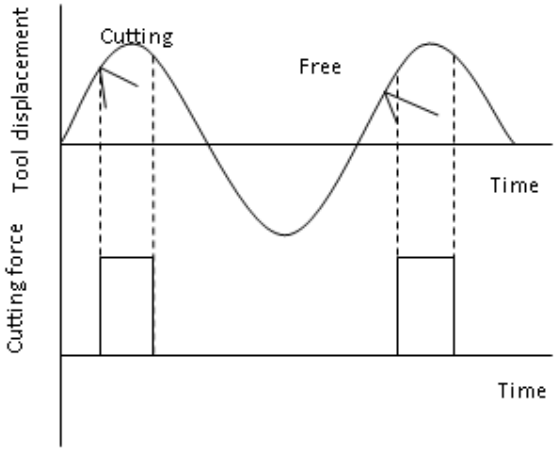

Figure 2.1 Pulse cutting state in the UVC method (Nath and Rahaman [22])

Jiao et al. [26] experimentally studied both ultrasonic and conventional assisted turning of quenched steel and found that surface micro-geometrical characteristics in ultrasonic assisted turning are better than that of conventional turning, especially when adopting lower machining speed; ultrasonic assisted turning of quenched steel is much easier to realize turning instead of grinding.

Lacalle et al. [27] experimentally studied both ultrasonic and conventional assisted turning of mild steel and found that surface roughness and tool temperature decrease and a tool life increase as compared to conventional turning (CT).

2.2.2 Finite element study on ultrasonic assisted turning

FEM is the major computational tool for simulation of the tool work-piece interaction in orthogonal cutting. From literature review of FE models on turning, it is found that major works are carried out by Childs et al. [28] and Trent and Wright [29] on conventional turning. A number of three dimensional finite element models for CT are developed and used to study forces in the tool; temperature, stress and strain distribution in the cutting zone and chip formation mechanism (Ceretti et al.[30], Anagonye and Stephenson[31], Pantel et al.[32] and Strenkowski et al.[33]).

Ramesh et al. [34] developed a three dimensional finite element model using isotropic materials and study the effect of the convective heat transfer. Pantale et al. [32] introduced another 3D model and that took into account dynamic effects, thermo mechanical coupling, constitutive damage law and contact with friction and its effect on the cutting forces and plastic deformation.

Mitrofanov et al. [35] first developed a 2D finite element model to understand the mechanics of the tool-chip interaction in vibration assisted turning and also analyzed distributions of stresses and strains in the cutting region, process of heat transfer in the work-piece material and in the cutting tool as well as to determine cutting forces and also Mitrofanov et al. [36-37] compared the CT and UAT methods numerically.

Mitrofanov et al. [38] also studied numerically the effect of lubrications in UAT method using 2D and 3D finite element models. It was demonstrated that the chip formed in lubricated UAT process was significantly more curled than the one produced in dry cutting. Ahmed et al. [39] investigated the thermally induced strains and residual stresses in the surface layer of the work-piece machined with UAT and CT.

Amini et al. [40] studied machining forces and stresses when turning IN738 with a tool vibrating at ultrasonic frequency and find the effect of process parameters using commercial package software Ansys® and MSC-Marc® and found improvement with an increase in the ultrasonic vibration amplitude and cutting speed. They also found that clearance angle has no significant effect on the magnitude of the machining force, but higher forces are produced with smaller tool rake angles. Conical–cylindrical aluminum vibratory tool with concentrically attached tool insert deliver more suitable performance.

2.2.3 Review on experimental set-up

The development and market demand for vibration cutting tool changed rapidly when more and more researchers enhanced the piezo-actuator in their machine design on the shop floor. Klocke et al. [18, 41] developed an ultrasonic assisted turning system using diamond cutting tool in Frauhofer institute for investigation focused on hard and brittle material (glass and steel) as shown in Figure 2.2.

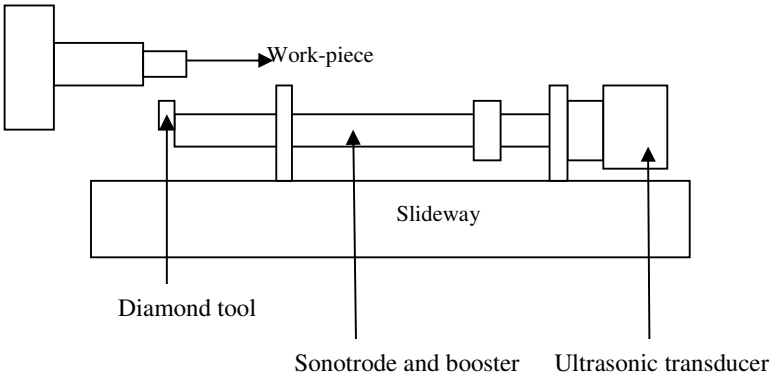

Figure 2.2 Ultrasonic assisted cutting system design by Frauhofer Institute [18, 41]

Masahiko and Murakawa [11] designed and developed a bolted type Langavin type transducer with nominal frequency of 21 kH_Z and power of 1 kW to generate ultrasonic vibration (Figure 2.3). Their investigation is focused on chipping and surface quality of UAT as compare to CT method.

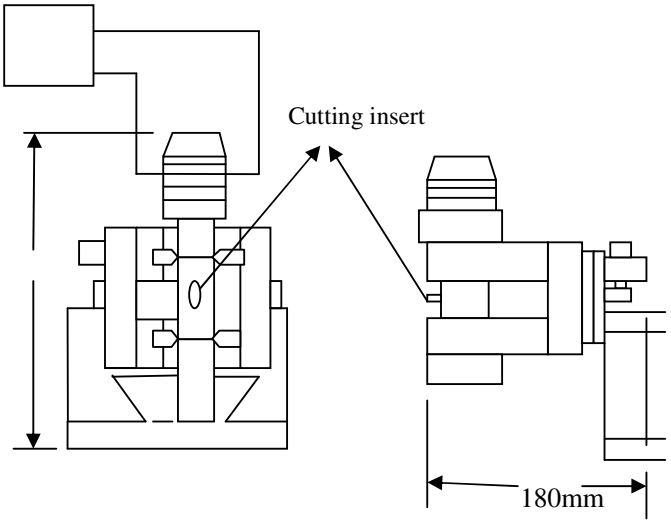

Figure 2.3 Practical ultrasonic vibration cutting tool system designed by Nippon Institute of Technology, Japan (Masahiko and Murakawa[11])

Babitsky and his co-workers [10], at Wolfson School of Mechanical and Manufacturing Engineering, Loughborough University, UK, developed an auto resonant ultrasonic turning system (Figure 2.4) using a commercially ultrasonic piezoelectric transducer for self tuning the system to keep the resonant mode of oscillations under variable conditions. The vibration of tip is measured by laser vibro-meter and the signal is processed by phase shifter, limiter and band pass filter to from an autoresonant control. The total system is controlled by a control system (PC). He also discussed about clamping method of the system. Clamping method used securing the inserts to the transducer is very important in order to obtain maximum amplitude of vibration at the tool tip. He also stated that external weight added to the system had some impact on the system.

Zhong et al. [20] devised a vibration device (Figure 2.5) for vibration assisted turning at school of mechanical and production engineering, NTU, Singapore. They used a lead-zincronate-titanium type piezoelectric transducer. The device not only holds the transducer firmly but also minimizes degree of freedom. He also discussed about the importance of one dimensional translation movement because undesired movements affects turning results.

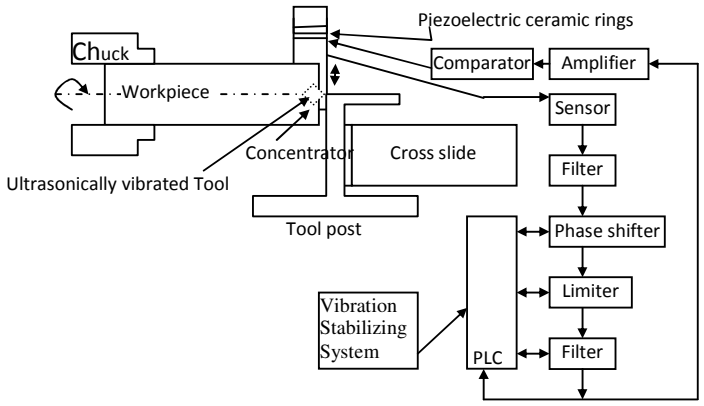

Figure 2.4 An auto resonant ultrasonic turning system designed by Wolfson School of Mechanical and Manufacturing Engg, Loughborough University, UK, (Babitsky et al.[10])

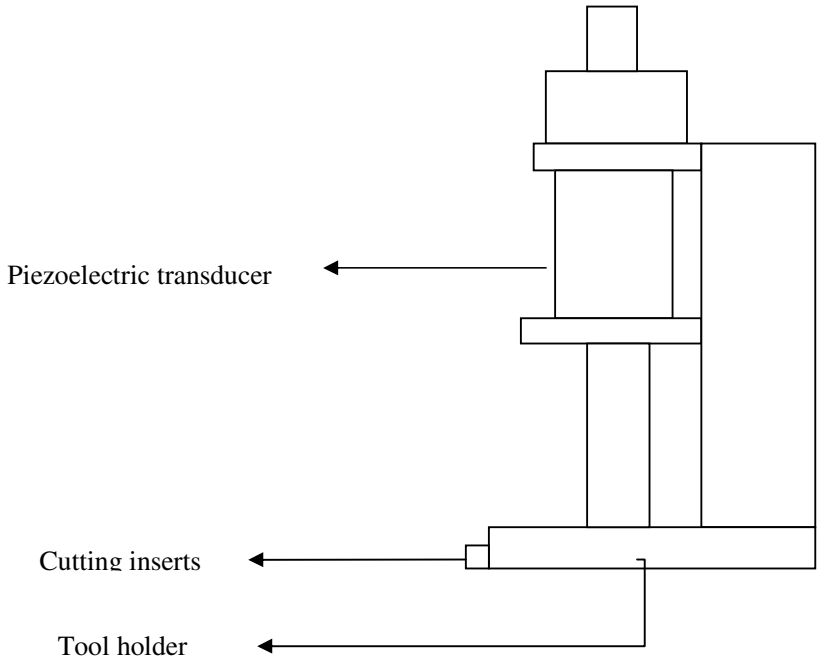

Figure 2.5 The vibration device designed by School of Mechanical and Production Engineering Nanyang Technology University, Singapore (Zhong and Lin [20])

2.3 Some Other Vibration Assisted Cutting

Adachi and Arai [42] developed an electronic servo that vibrates in low frequency up to 1000 Hz. On their experimental study using aluminum work-piece for drilling and they found that burr size could be reduced considerable with the assistant of vibration cutting. They built their servo machine on the spindle of the NC milling machine. A benefit of this design is the simplicity with which it can be modified for different applications. The idea of their work was to develop a technique applicable to the drilling process for surface-roughness measurement in the wall paths.

Wu and Fan [43] developed a centre less grinding technique called the ultrasonic elliptic-vibration shoe centre less grinding. This new method employs an ultrasonic elliptic-vibration shoe to hold up the work-piece and control the work-piece rotational motion instead of using a modifiable wheel such as that employed in conventional centre less grinding. The vibration ellipse is applied into the shoe or bed of the work-piece with frequency of 20 kHz. The shoe is given an intermittent force in micron scale to push the cylindrical work-piece towards a spot between the bed and the grinding wheel. They discovered the rotation of the work-piece was controlled by the friction force between the work-piece and the shoe so that the

peripheral speed of the work-piece is the same as the bending vibration speed on the shoe end-face. On the other hand, the geometry or roundness of the work-piece can be controlled by tilting the two angles for shoe and for bed-piezo.

2.4 Cutting Mechanism of One Dimensional Ultrasonic Assisted Cutting

The one dimensional ultrasonic cutting, the tool in one plane parallel to the work-piece surfaces so as inline to the principal cutting force as shown in Figure 2.6. Figure 2.6 shows the kinematic of one dimensional ultrasonic assisted cutting where the tool drives in a linear path subjected to the vibration frequency and vibration amplitude. It has been used by Shamoto [1], Kumbabe [3], Moriwaki [8] and Isaev et al. [12] in their early respective investigations of ultrasonic assisted machining.

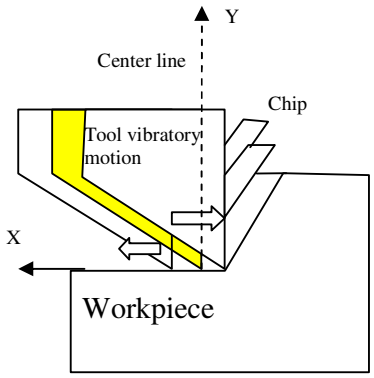

Figure 2.6 One dimensional vibration assisted cutting (Shamato, [1])

The alternating get-in-touch with of tool rake face relative to the work-piece is expressed as:

$$x = a\sin\omega t + Vt \tag{2.1}$$

$$\frac{\partial x}{\partial t} = a\omega\cos\omega t + V \tag{2.2}$$

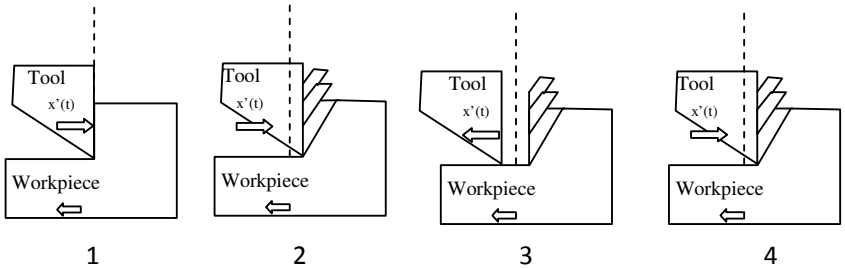

Figure 2.7 One dimensional vibration assisted machining [37]

Where x(t) and $\frac{\partial x}{\partial t}$ are the instantaneous position and velocity at time t, a is the amplitude of the tool vibration, f is the vibration frequency, and angular frequency $\omega = 2\pi f$. In Figure 2.7 (1&2) the tool velocity is in positive direction and work piece velocity is in negative direction. At position 1 the tool rake face has just come into contact with the uncut material and in position 2 the tool has cut the material. In position 3 the velocity of tool and work-piece is same direction and the velocity of tool is more than the velocity of work-piece that's why the tool is withdraw from the work piece and in position 4 the tool and work-piece again in opposite direction and procedure of cutting is a cyclic process in which tool is contact and withdraw from the work-piece surface, which gives better surface finish and improvement of tool life etc in ultrasonic assisted cutting.

Brehl and Dow [44] reviewed the vibration assisted machining in 1D (linear vibratory tool path) and 2D (circular/elliptical vibratory tool path) and described the periodic separation between the tool rake face and uncut material. They found that characteristic of vibration assisted machining is related to observed reductions in machining forces and chip thickness. The reduced tool forces in turning are related to improvements in surface finish and extended tool life. They believed that the intermittent cutting characteristic reduces the effect of thermo-chemical mechanisms during turning and responsible for rapid wear of diamond tools when machining ferrous materials. This feature of vibration assisted machining increases its ability to machine brittle materials in the ductile regime at increased depth of cut.

2.5 Summary

This chapter has presented a literature survey with a critical review on one dimensional ultrasonic assisted turning. Different ultrasonic assisted turning setup, previous experimental and finite element studies on ultrasonic assisted turning has been discussed. The mechanism of one dimensional ultrasonic assisted turning is also discussed.

The previous works presented are adapted and improved to produce a novel idea in ultrasonic assisted turning system development and its applications by using piezo-actuator as a vibration generator. Experiments have been conducted and obtained data are analyzed statistically.

Chapter-3

Design and Finite Element Modeling of Ultrasonic Vibratory Tool (UVT)

CHAPTER 3

DESIGN AND FINITE ELEMENT MODELING OF UVT

3.1 Ultrasonic Vibratory Tool

Ultrasonic vibratory tool (UVT) is an element operating in a longitudinal mode used for efficient transfer of ultrasonic energy from a source element (transducer) to a second horn, coupler, tool, or load. Equivalently, it is a transmission line, generally (but not always) providing a change of amplitude of vibration between the input and the output ends of the horn. The main purpose of the horn is to provide amplitude of vibration at its output end that is greater than that at the input end. Thus this is the critical link in the UAT.

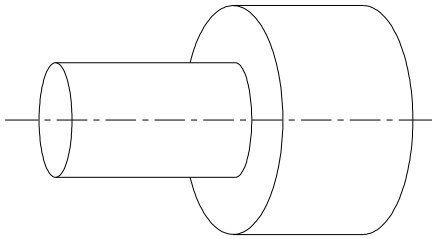

a) Stepped vibratory tool

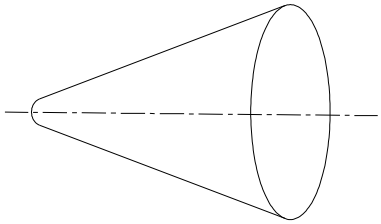

b) Conical vibratory tool

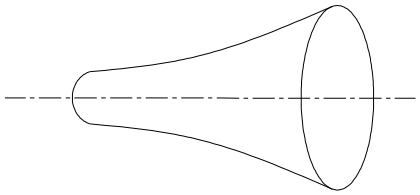

c) Exponential vibratory tool

Figure 3.1 Different types of vibratory tool

This has got several names like mechanical focusing device, shank, velocity transformer, concentrator, amplifier etc. The ultrasonic vibratory tools are specially shaped to provide a reduction in cross section at the driven end. Ultrasonic vibratory are generally made of metals that have high fatigue strengths and low acoustic losses and they should be easily brazed or soldered. The metals most often used to construct ultrasonic vibratory tool are monel, titanium, stainless steel, heat treated steel and aluminium. Ultrasonic vibratory tools can be manufactured in various shapes and dimensions, the most common shapes being shown in Figure 3.1.

3.2 Vibratory Tool Equation and its Specific Solution

3.2.1 Plane wave equation

Let us consider the motion of plane wave in a velocity of sound, C, and attenuation of the waves is assumed to be zero. The waves are free to move in both the positive and negative directions of X-axis as described by equation (3.1)

$$\xi = f_1(x - ct) + f_2(x + ct) \tag{3.1}$$

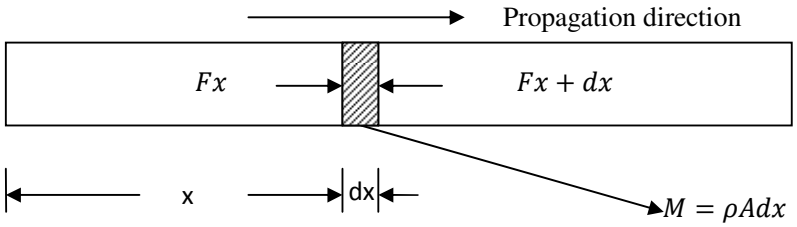

Figure 3.2 Forces on an increment normal to the direction of propagation of a longitudinal plane wave in a uniform slender bar

Where $f_1(x\text{-}ct)$ refers to waves moving in the positive direction of X-axis and $f_2(x+ct)$ to waves moving in the negative direction of X-axis. ξ is the displacement of dx . If $f(x\text{-}ct)$ and $f(x+ct)$ are continuous, equation 3.1 may be differentiated twice with respect to x (keeping t constant), giving

$$\frac{\partial^2 \xi}{\partial^2 x} = f_1''(x - ct) + f_2''(x + ct) \tag{3.2}$$

Similarly, differentiating equation 3.1 with respect to t (keeping x constant)

$$\frac{1}{C^2}\frac{\partial^2 \xi}{\partial^2 t} = f_1''(x - ct) + f_2''(x + ct) \tag{3.3}$$

By comparing equations (3.2) and (3.3),

$$\frac{\partial^2 \xi}{\partial^2 t} = C^2 \frac{\partial^2 \xi}{\partial^2 X} \tag{3.4}$$

The equation 3.1 is the general solution of plane wave equation 3.4. The characteristics of a true plane wave are that pressure and motions at every position in a plane normal to the

direction of propagation are equal in amplitude and phase. The kind of wave is not defined by the velocity 'C' in equation 3.4. The bar is assumed to be so slender ($D \gg \lambda$) that the effects of poison's ratio can be neglected is a specific example of equation 3.4. Where λ the wavelength and D is is the diameter of the bar.

Let us consider a uniform, narrow, homogeneous, elastic bar as being composed of series of incremental elements of density ρ, longitudinal thickness dx, and cross section area A (Figure 3.2). Losses are assumed to be negligible. Balancing the forces of momentum of an element

$$F_m = Ma_c = \rho A \frac{\partial^2 \xi}{\partial x^2} dx \tag{3.5}$$

Where, $M=\rho A dx$, ξ is displacement of the element dx, $a_c = \frac{\partial^2 \xi}{\partial x^2}$ and t is the time against the elastic reaction of a neighboring element situated between x and (x+dx), in the same way using deriving spring equation,

$$F_{spring} = EA \frac{\partial^2 \xi}{\partial x^2} dx \tag{3.6}$$

$$F_x = -EA\frac{\partial \xi}{\partial x} \qquad F_{x+dx} = dF_x \frac{dF_x}{dx} dx$$

From Figure 3.2 $F_m=F_{spring}$,

So $$\rho A \frac{\partial^2 \xi}{\partial x^2} dx = EA \frac{\partial^2 \xi}{\partial x^2} dx \tag{3.7}$$

or $$\frac{\partial^2 \xi}{\partial t^2} = \frac{E}{\rho} \frac{\partial^2 \xi}{\partial x^2} = c^2 \frac{\partial^2 \xi}{\partial x^2} \tag{3.8}$$

Where $$C = \sqrt{\frac{E}{\rho}} \tag{3.9}$$

C is the velocity of sound and E is young's modulus of elasticity in the medium of the bar.

3.2.2 Plane wave equation of tapered horn

Similarly, the wave equation of tapered horn (Figure 3.3) in terms of particle displacement, ξ is,

$$\frac{1}{C^2}\frac{\partial^2 \xi}{\partial t^2} - \frac{1}{A}\frac{\partial A}{\partial x}\frac{\partial \xi}{\partial x} - \frac{\partial^2 \xi}{\partial x^2} = 0 \tag{3.10}$$

And in terms of particle velocity, v, and implying harmonic motion,

$$\frac{\partial^2 v}{\partial x^2} - \frac{1}{A}\frac{\partial A}{\partial x}\frac{\partial v}{\partial x} - \frac{\omega^2}{C^2} = 0 \tag{3.11}$$

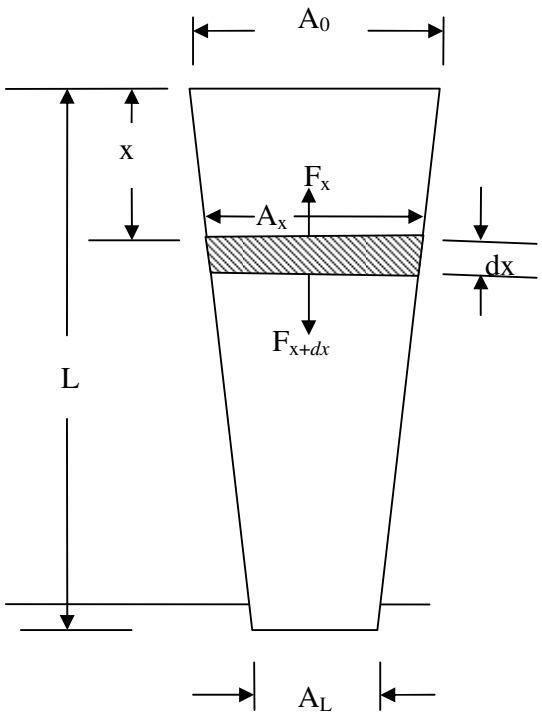

Figure 3.3 Propagation of longitudinal wave in a tapered horn

3.2.3 Plane wave equation of stepped cylindrical horn or vibratory tool

For uniform cross section bar $\frac{\partial A}{\partial x} = 0$,

the equation of tapered bar(equations 3.10 & 3.11) reduces to the plane wave equation for which the general solution, in terms of the displacement, ξ, will be

$$\xi = \left[A\cos\frac{\omega x}{c} + B\sin\frac{\omega x}{c} \right]\cos(\omega t) \tag{3.12}$$

or in terms of particle velocity

$$v = -\omega\left[A\cos\frac{\omega x}{c} + B\sin\frac{\omega x}{c} \right]\sin(\omega t) \tag{3.13}$$

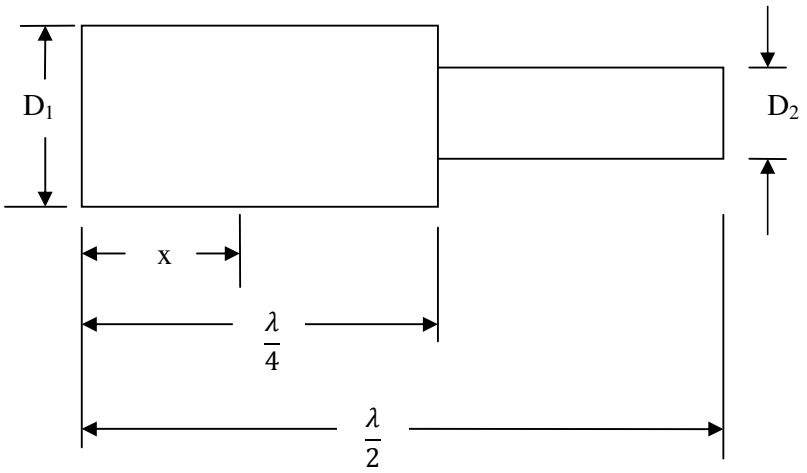

Figure 3.4 Stepped cylindrical half wave vibratory tool

For longitudinal half wave uniform bar (Figure 3.4)

$$\xi = \xi_M \cos\left(\frac{\omega x}{c}\right)\cos(\omega t) \tag{3.13}$$

$$v = -\omega\xi_M \cos\left(\frac{\omega x}{c}\right)\sin(\omega t) \tag{3.14}$$

where ξ_M is a maximum displacement and is located at x=0.

The acceleration at any point, x, along the tool is

$$a = -\omega^2\xi_M \cos\left(\frac{\omega x}{c}\right)\cos(\omega t) = -\omega^2\xi \tag{3.15}$$

where λ is the wave length, ω is the angular velocity.

Stress, s, at x in a half wave resonant bar is

$$s = \frac{iE}{\omega}\frac{dv}{dx} \tag{3.16}$$

Where $\omega\xi_m$ is the maximum velocity and occurs at X=0,E is young's modulus of elasticity, and $i = \sqrt{-1}$.

For the vibratory tool (Figure 3.4), with the step occurring at the mid plain along the length, momentum of the elements on either side of step leads to the identity

$$\frac{\xi_1}{\xi_2} = \frac{v_1}{v_2} = \frac{A_2}{A_1} \tag{3.17}$$

Where ξ_1 & ξ_2 are particle displacements (amplitudes), v_1 & v_2 the particle velocities, A_1&A_2 are the cross sectional areas at x= 0 and x=L.

or,
$$\xi_1 = \frac{A_2}{A_1}\xi_2 \tag{3.18}$$

ξ_1 & ξ_2 are the amplitudes at driving and driven end of the vibratory tool.

3.2.4 Stress concentration at a step in horn

When double cylinders are used as a half wave vibratory tool with step at the node (λ/4), the maximum stress occurs at the step is calculated approximately by using the stress occurs at the step. The maximum stress is calculated approximately by using the stress in the smaller diameter sector. The stress at node is

$$s_m = E\frac{\omega\xi_1}{X\xi_2} = E\frac{\omega}{C}\frac{A_2}{A_1}\xi_1 \tag{3.19}$$

A horn designed according to Figure 3.4 will fail in fatigue at the junction between the two elements. This junction is a position of maximum stress, and abrupt change in diameter increases the stress near the surface of the smaller diameter segment and the nodal face of the larger diameter. In practice, these horns are designed with a highly polished fillet located between the larger diameter and the smaller diameter segments to reduce the stress concentration at the junction. The concentration value, K, (Table 3.1) for various fillet radii can be determined by using the relationship [45] (Figure 3.5)

$$K = K_1 + K_2\left(\frac{2h}{D}\right) + K_3\left(\frac{2h}{D}\right)^2 + K_4\left(\frac{2h}{D}\right)^3 \tag{3.20}$$

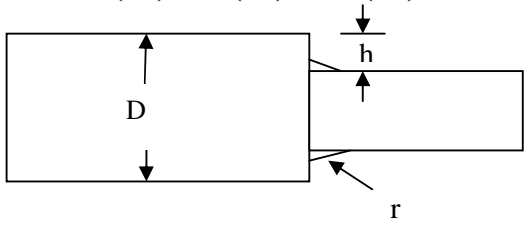

Figure 3.5 Double cylinders with square shoulder and fillet

Table 3.1 Concentration value (K) for various fillet radii

	For $0.25 \ll h/r \ll 2.0$	For $2.0 \ll h/r \ll 20.0$
K_1	$.927+1.149(h/r)^{0.5}-0.086h/r$	$1.225+0.831(h/r)^{0.5}-0.010h/r$
K_2	$0.011-3.029(h/r)^{0.5}+0.948h/r$	$-1.831-0.318(h/r)^{0.5}-0.049h/r$
K_3	$0.304+3.979(h/r)^{0.5}-1.737h/r$	$2.236-0.522(h/r)^{0.5}+0.176h/r$
K_4	0.366-2.098(h/r)0.5+0.875h/r	-0.630+0.009(h/r)0.5-0.117h/r

The concentration stress, s_c, is

$$s_c = Ks_m \tag{3.21}$$

Where s_m is the values of stress calculated using equation 3.19.

3.2.5 Calculation of nodal plane in stepped cylindrical vibratory tool.

Locations of nodal planes are necessary to clamping the ultrasonic system. The plane where particle displacement of vibratory tool is zero is called nodal plane. For rigidity of the ultrasonic system it is better to clamp at nodal plane. Clamping the ultrasonic system other than nodal plane fluctuate the amplitude and frequency of the ultrasonic vibratory tool which affect the ultrasonic assisted tuning (UAT).

Referring equation 3.13

$$\xi = \xi_M \cos\left(\frac{\omega x}{c}\right)\cos(\omega t) = 0 \tag{3.22}$$

(At nodal plane ξ=0)

It implies,

$$\cos\left(\frac{\omega x}{C}\right) = 0 \tag{3.23}$$

$$x_n = \frac{nC}{4f} \quad \text{(n=odd number)} \tag{3.24}$$

Where x is nodal plane position, f is frequency and C is velocity of sound.

3.3 Finite Element Modeling of Ultrasonic Vibratory Tool

3.3.1 The finite element

The finite element is the basic unit of analysis in an FE problem. The entire structure under consideration is a group of finite elements with continuity of displacements and equilibrium of stresses maintained at the nodes belonging to a individual element. The solution of the problem becomes one of matrix algebra, which provides efficient numerical calculation.

3.3.2 Finite element modeling

FEA has been used for more than 50 years to various structural, thermal, and acoustic problems. In this present problem ANSYS® software package is used to analyze dynamic analysis of ultrasonic vibratory tool. Both modal and harmonic analysis of UVT are carried out to calculate the natural frequency and amplitude of tool.

3.3.2.1 Geometrical modeling

The geometry (Figure 3.7) is generated in preprocessor modeling. The length of the horn is the resonance length (120.75mm).The input and output diameter is 40 and 20mm and fillet dimension (h/r) is taken 2 (Table 3.1).

3.3.2.2 Material properties

The titanium is used as the horn material for the analysis with properties, elastic modulus E= 110 GPa, Poisson ratio, γ=0.33, mass density ρ = 4700 Kg/m^3.

3.3.2.3 Element type selection

Selection of suitable element types according to material and design of the UVT are made to ensure the analytical correctness. The UVT is predominantly divided into metallic materials. Element selection varies due to differing features. Considering the special curved surface structure of the vibrating system, solid 92, a tetrahedron with 10 nodes (Figure 3.6) is selected as the element. As the tetrahedron element allows the finite element analysis software to grid a complex geometric model easily, it is considered to be suitable for the shape requirement of the vibrating tool.

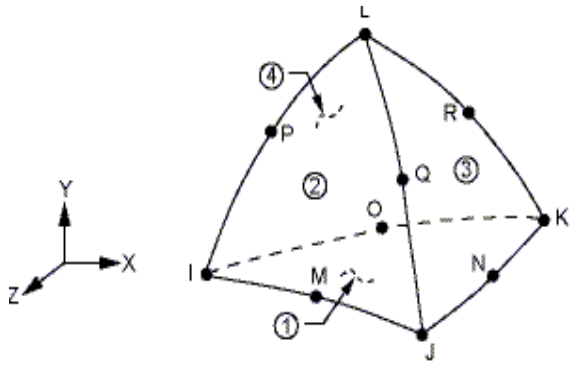

Figure 3.6 Solid 92 elements [Reproduced from ANSYS® 12.0 user guides [46]]

3.3.2.4 Mesh generation

According to the basic principles of finite element analysis theory, the smaller the mesh element size is, the more accurate the results of an analysis will be. If the mesh element sizes infinitely small, the theoretical model will approach the optimal solution. However, this is only a presupposition. In the analysis process, when elements are too small, element meshing generates too many elements, nodes and freedom for the model in general. This increases computational intensity, resulting in a model that is either too time-consuming to solve, or potential errors in values. Thus, reasonable mesh element size (number of elements) is a factor that should be considered in a finite element analysis. 14491 numbers of elements with 21517 nodes are used for the model in the present analysis.

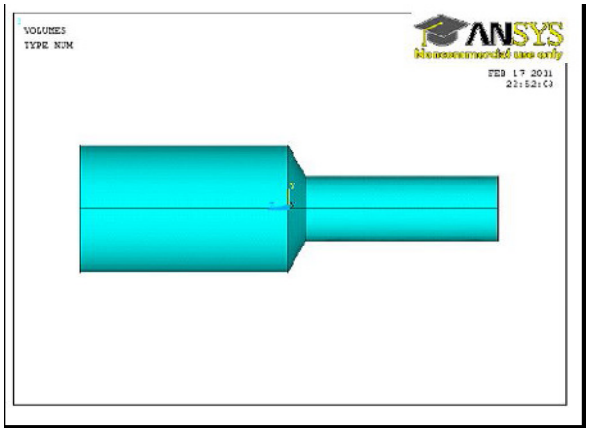

Figure 3.7 Geometry generation of UVT

3.3.2.5 Boundary condition

After finalizing settings for the ANSYS® pre-processor, boundary conditions are provided to the solution-finding processor. The output of piezoelectric transducer is applied as input of tool. 0.01mm uniformly distributed displacement load is applied at the big end of the ultrasonic vibrating tool as shown in Figure 3.8.

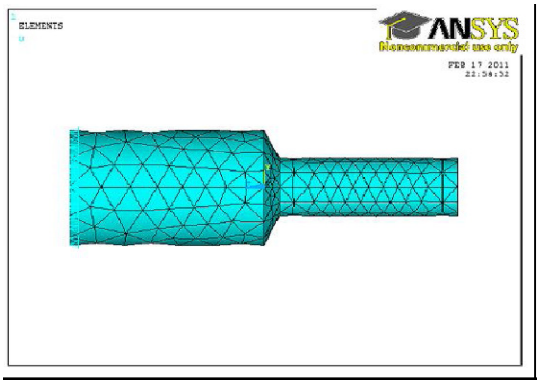

Figure 3.8 Displacement load applied at big end

3.4 Results and Analysis

3.4.1. Modal analysis

Modal analysis allows the design to calculate resonant vibrations or to vibrate at a specified frequency. It helps in calculating solution controls for other dynamic analyses, because a structure's vibration characteristics determine how it responds to any type of dynamic load; always perform a modal analysis first before trying any other dynamic analysis. Modal analysis is a linear analysis, any nonlinearities such as plasticity and contact elements, are ignored, even if they are defined. Several mode extraction available in the modal analysis but in present case BLOCK LANCZOS method is selected.

3.4.2 Harmonic analyses

The technique to determine the steady state response of a structure to sinusoidal (harmonic) loads of known frequency where the input harmonic loads are forces, pressures, imposed displacements, and imposed voltage of known frequency. The output parameter is harmonic displacement at each DOF, current flow for piezoelectric elements, stresses and strains.

3.4.3 Finite element analysis of ultrasonic vibratory tool

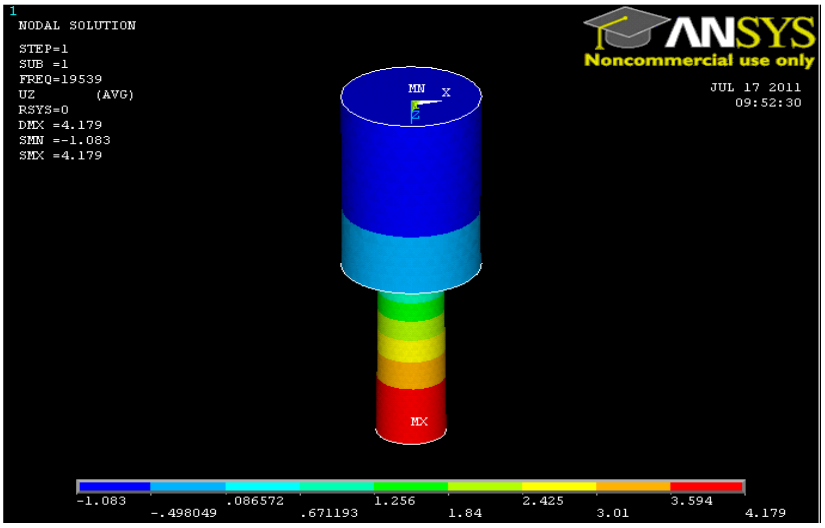

Figure 3.9 Modal analysis of UVT (mode 1)

There are numbers of resonant frequencies recorded (Table 3.2). The longitudinal axial mode shape of UVT is at 19539Hz as shown in Figure 3.9. There are also other modes (Table 3.2) around longitudinal mode at 22791 Hz and 22799 Hz shown in Figures 3.10 and 3.11. It is clear from Figures 3.10 and 3.11 cause a bending mode superimposed on the main longitudinal mode of ultrasonic vibration. This is an undesirable phenomenon which can jeopardize the advantages of UAT such as worst turning operation. The frequency response functions (FRF) of UVT is shown in Figure 3.12 which shows that the amplitude is maximum at resonance frequency 19539Hz. The natural frequency 19539Hz is also within the working frequency range of the generator (19,500Hz-20,000Hz).

From harmonic response analysis shown in Figure 3.13, it is clear from figure that the working amplitude of the tool is 0.039234 mm when the driving amplitude is 0.01 and the result found from ANSYS® is nearly equal to the theoretical result 0.04 (Eq. 3.17) and the nodal plane is located at mid section of the UVT which is also good agreement with theoretical result. The percentage of error between theoretical and ANSYS® is 1.9% (Table-3.2).

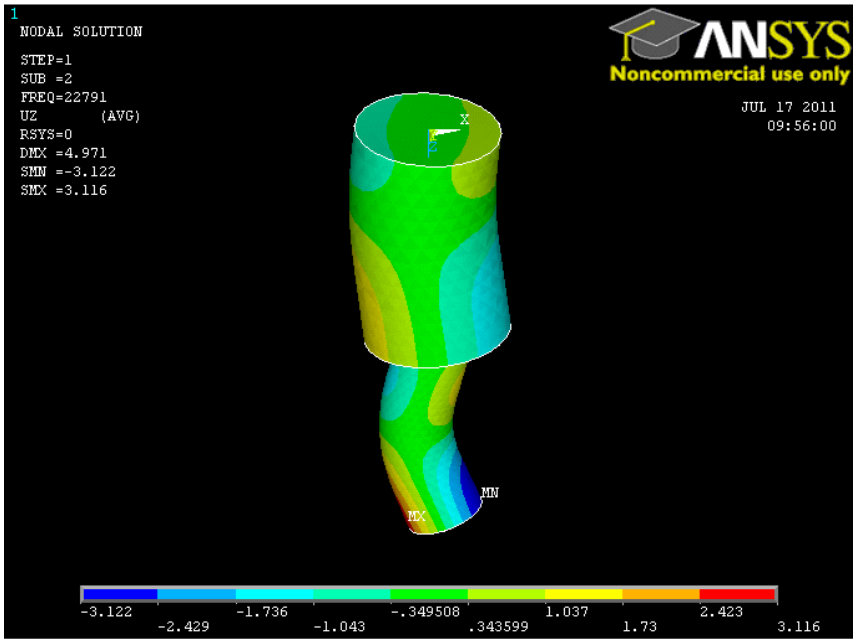

Figure3.10 Modal analysis of UVT (mode 2)

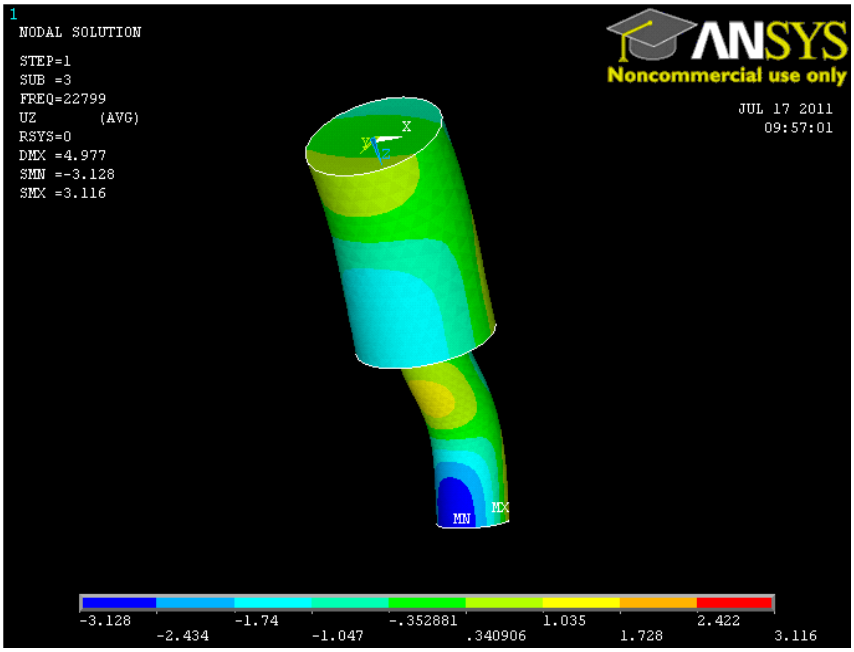

Figure 3.1 Modal analysis of UVT (mode 3)

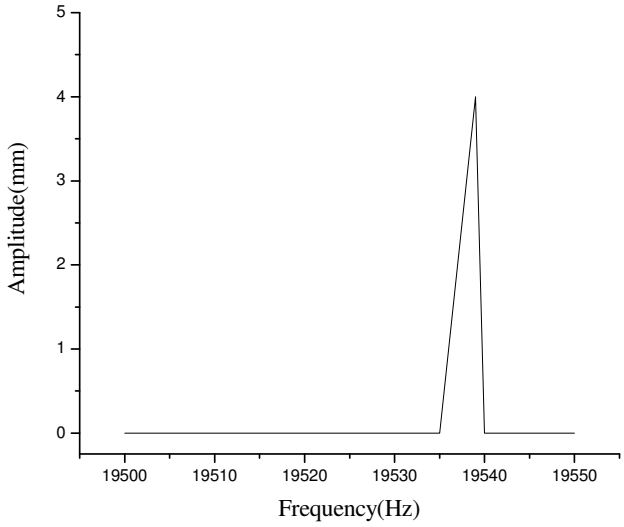

Figure 3.12 Frequency response function of UVT

Table3.2 Dynamic Analysis of UVT

Mode	Natural Frequency (Hz)	Figure
1	**19539**	**3.8**
2	22791	3.9
3	22799	3.10

Horn material			Titanium					
D_1 (mm)	D_2	Fillet dimension (h/r)	Resonance length	Driving amplitude	Nodal point x_n	Amplitude at working end (theoretical)	Amplitude at working end (ANSYS®)	% of error
20mm	10mm	2	120.75mm	0.01mm	60.375mm	0.04mm	0.039234mm	1.9

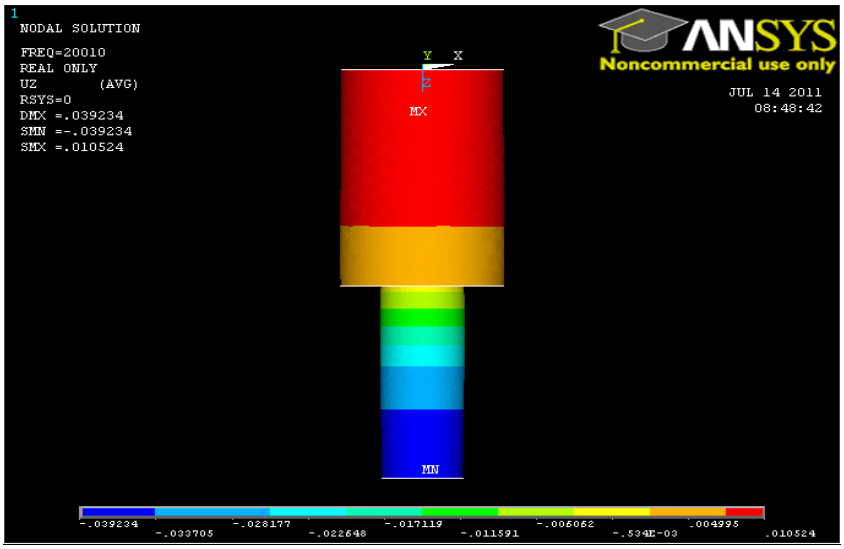

Figure 3.1 Harmonic response analysis of UVT

3.5 Conclusions

It is very important to know the amplitude of vibration at every point of the ultrasonic horn, because: it allows precise determination of the nodal plane position for clamping; gives exact displacement value at tool-workpiece contact points which depend on amplitude at the top of the horn; tests various shapes of ultrasonic horns before manufacturing a real prototype.

The results of modal analysis show that used horn configuration gives definite and wide nodal band for clamping purpose. An additional point to be considered when designing UAT setup is that the horn should have at least one natural frequency within the allowable ultrasonic frequency, in this case 19539 Hz (19,500–20,500 Hz). It can be concluded that the geometrical dimension and material properties of UVT used in analysis of horn can deliver the required frequency. This frequency matches with other part of the ultrasonic system and the resonance frequency of the horn under the generator frequency and the UVT is amplified 4 times of source amplitude to working amplitude.

Chapter-4

Experiment

CHAPTER 4

EXPERIMENT

4.1 Calculation of Tool Tip Amplitude

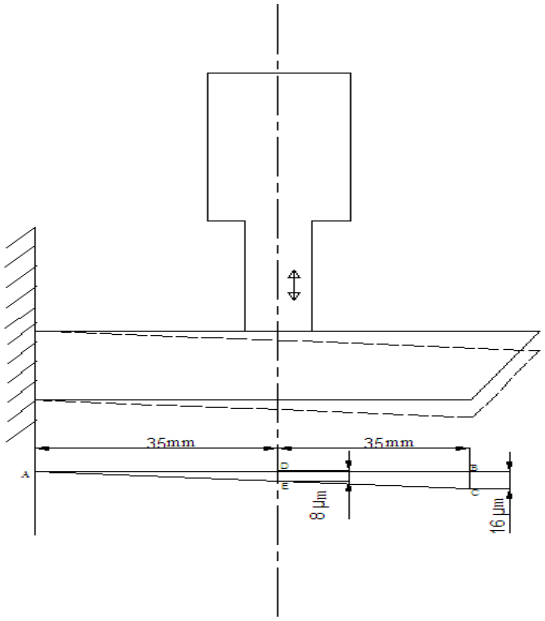

Figure 4.1 Cutting tool during ultrasonic vibration (treated as a cantilever beam)

As shown in Figure 4.1 and Figure 4.2 the cutting tool treated as a cantilever beam in this experiment. The vibratory tool is placed 35mm from the fixed end and cutting tip is 70mm from the fixed end. The output amplitude of vibration of UVT is 8µm.

From Figure 4.1 (using triangular rule)

$$\triangle DAE \cong \triangle ABC$$

or $$\frac{BC}{DE} = \frac{AB}{AD}$$

or $$BC = \frac{AB}{AD} DE$$

$$BC = 16\mu m$$

BC is the amplitude of vibration of cutting tip.

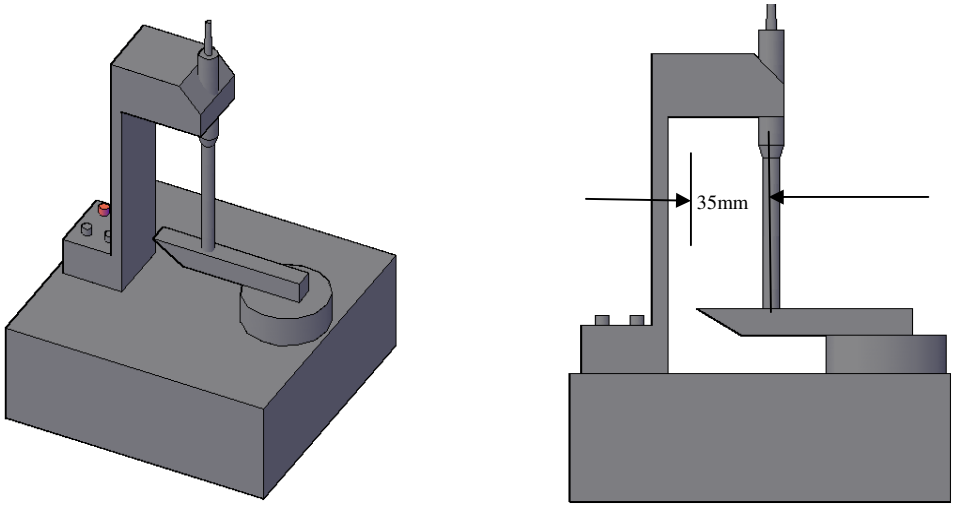

Figure 4.2 3D views of experimental setup (Cutting tool treated as cantilever beam)

4.2 Experimental Setup and Procedures

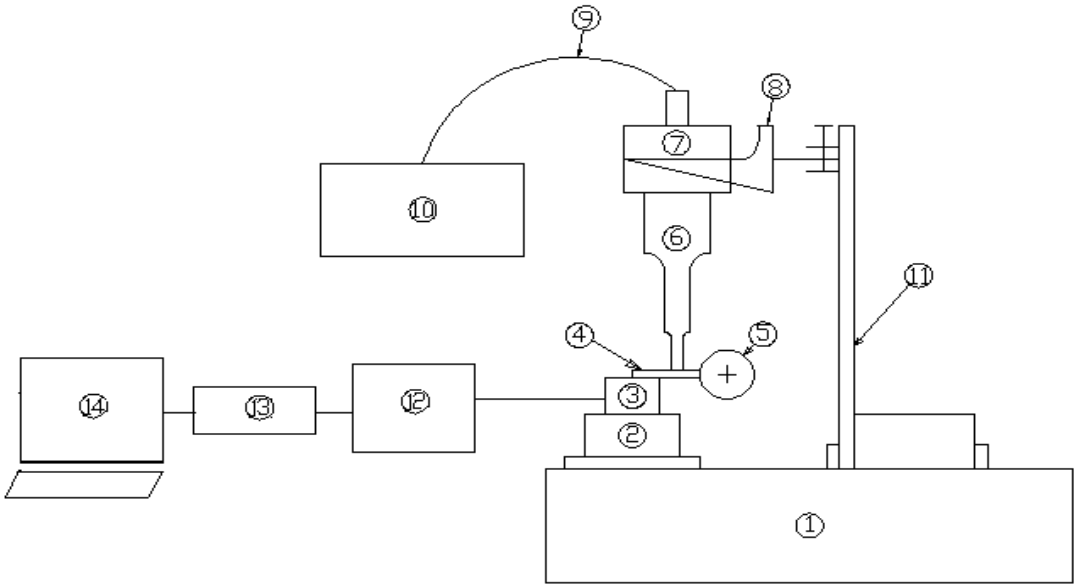

Figure 4.3 Schematic diagram of ultrasonic assisted turning system

1. HMT Model NH 26 Lathe.
2. Compound plate
3. Dynamometer (Kistler model 9272)
4. Tool (treated as a cantilever)

5. Work-piece
6. Ultrasonic vibratory tool (UVT)
7. Booster/converter
8. Bracket
9. H.F.Cable with 4 pin coaxially (M) to (F) connector connects 20 kHz high voltage to converter.
10. Generator
11. L-type holder
12. Charge amplifier model 5070A
13. DAQ
14. PC (CONTROL UNIT)

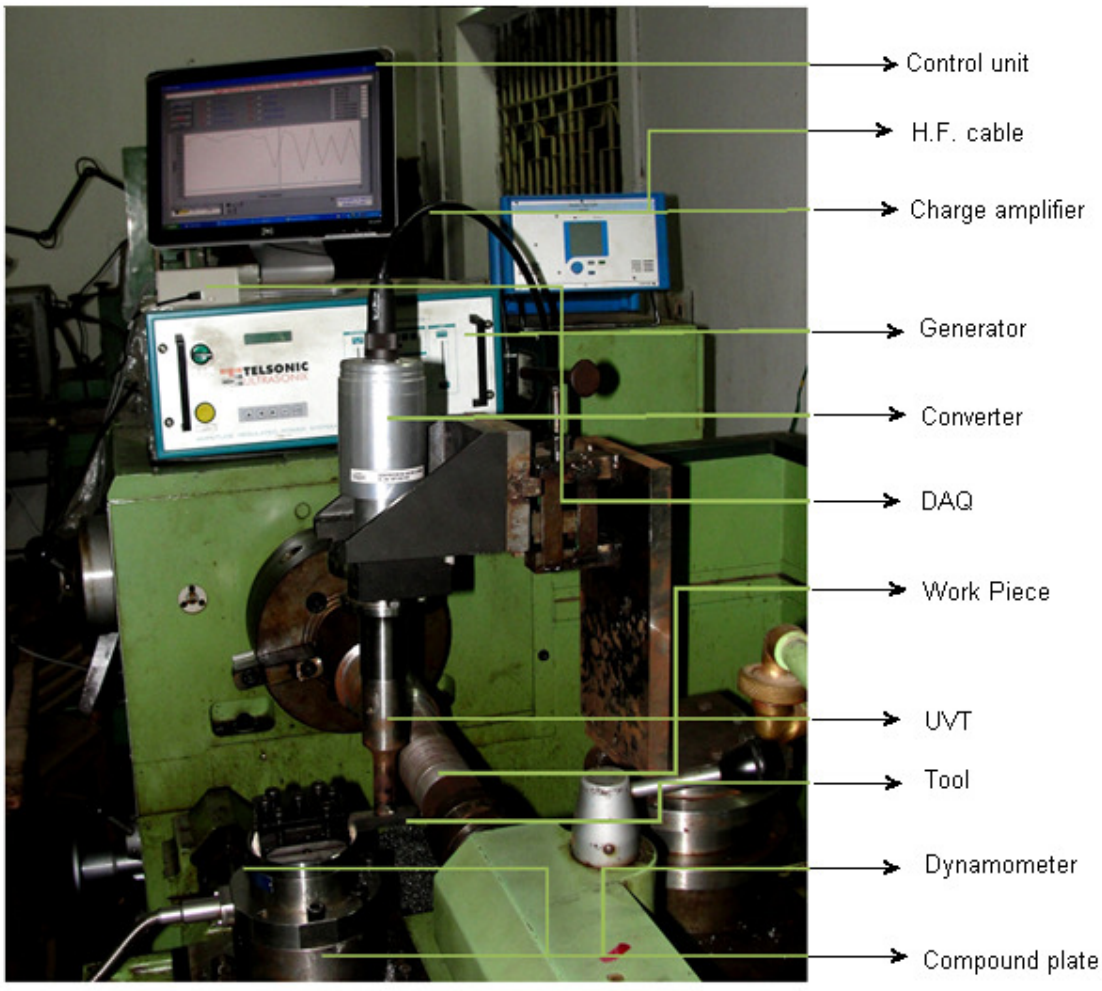

Figure 4.4 Experimental setup

Figure 4.5 Lathe by which all experiments are performed (HMT Model NH 26)

Table 4. 1 Composition of specimen (carbon steel)

c	Si	Mn	P	S	Cr	Mo	Ni
0.75%	0.01%	1.141%	0.072%	0.307%	0.75%	0.006%	0.27%

Table 4. 2 Specifications Ultrasonic system

Line voltage	220V/230V AC Single phase
Input frequency	50 Hz
Current consumption	220V, 50Hz.-6A
Output frequency	20kHz
Amplitude	8µm
Output power	2kW
Output control	Auto tuning with load output power range 30 to 100% of nominal converter amplitude.
Operational mode	Continuous mode:-on/off & timer mode.
Tuning	Auto tuning operation in normal mode. Also manual tuning facility.
Converter weight with horn	Approx. 1Kg
Generator weight	Approx. 3Kg

Table 4. 3 Specification of cutting tool

Material	Rake angle	Clearance angle	Cutting edge angle	Nose radius
Tool steel	0^0	24.932^0	43.631^0	0.2mm

4.2.1 Description of experimental set-up

Figure 4.3 shows a schematic diagram of the ultrasonic vibration turning system used in the present experiments. As shown in Figure 4.4 the work-piece (Table 4.1) is clamped by the three jaw chuck of 'HMT model NH 26' lathe (Figure 4.4).The commercial piezoelectric transducer (unloaded 20±0.5 kHz frequency, Table 4.2) provides vibration to the ultrasonic vibratory tool (UVT). The tip of UVT is placed vertically on the cutting tool. The cutting tool (Table 4.3) is treated as a cantilever beam as shown in Figure 4.1, which is fixed on Kistler model 9272 dynamometer (Table 4.4) as shown in Figure 4.4. The UVT (Table 4.5) placed perpendicularly to the work-piece in the horizontal plane allows the cutting tool to make the ultrasonic vibration movement in the cutting velocity direction. The amplitude of vibration is 16μm at cutting tool tip as calculated (section-4.1), which is the working amplitude for all experiments.

The ultrasonic transducer is clamped at its nodal point by a light weight bracket and the bracket is fixed by sliding mechanism with special designed L-shape holder. This L-shaped holder maintained the height of the ultrasonic transducer, which is fixed on cross slide of the lathe. The UVT is connected to generator by H.F. Cable with 4 pin coaxially (M) to (F). The generator is generating high frequency around 20±0.5kHz with 2.0kW (max) power from the input mains voltage 230V AC, 50Hz frequency.

Table 4. 4 Specifications of Kistler model 9272 dynamometer

Measuring range	
Force/moment	Range
F_X	-5-5kN
F_Y	-5-5kN
F_Z	-5-5kN
M_Z	-200-200N-m

Table 4. 5 Specification of UVT

Material	Titanium
Geometry(D_1-D_2-L)	40mm-20mm-120.75mm
Young's modulus (E)	110 Gpa
Poisson's ratio (γ)	0.33
Density (ρ)	4700
Natural frequency(f)	19539Hz

Table 4. 6 Specifications of Data acquisitions (DAQ)

-National Instrument make USB based 14 bit 8 channels data card along with Labview based data acquisition software to acquire the necessary parameters in the range of +/- 5V. Model no-NI-DAQmx^{TM}8.9.5, Sampling rate 1000 per second

Table 4. 7 Specifications of control unit (PC)

Processor	Pentium 4
RAM	526MB
Screen resolutions	800×600 pixels
Operating system	Windows XP

4.2.2 Work piece preparation and processing

Figure 4.6 Work piece after machining operation

The work-piece is cylindrical and faces are machined prior to the experiments. A finishing cut with a very small depth of cut is performed using the same cutting tool to be used in the experiments, in order to eliminate any leftover eccentricity. In the experimental run, first cut is made conventional and as soon as the tool travelled by 10mm the vibration is switched on thus allowing the second cut to proceed under same cutting condition but with ultrasonic vibration. After finishing one experiment as shown in Figure 4.6, it is marked for identification. So, every experiment is divided two parts, first part is convention turning (CT) and second one is ultrasonic assisted turning (UAT). Each experiment was done at different cutting conditions and the same procedure is applied in different experiments.

4.2.3 Measurement of cutting force

The Kistler model 9272 dynamometer (Table 4.4) is used to measure the cutting forces during experiments. The cutting tool is fixed on dynamometer and the dynamometer is fixed on the cross slide of the lathe. The dynamometer measures the active cutting force regardless of its application point. Both the average value of force and the dynamic force increase may be measured. The typical measuring chain consists of a piezoelectric dynamometer with charge output, with connecting cable and the multichannel charge amplifier as well as a data acquisition (DAQ) (Table 4.6) and analysis system (Table 4.7) as shown in Figure 4.4.

4.2.4 Measurement of surface roughness

Surface quality was assessed by measuring surface roughness along the axial direction of the work pieces. Both surfaces produced by application of ultrasonic vibration, and under conventional conditions, are evaluated using the "HANDYSURF E-35A" surface measuring instrument. Centre line average (R_a) value is used to analyze the surface roughness of machined work-piece.

4.3 Experimental condition

4.3.1 Composition of the material

Carbon steel is chosen as work piece material for all experiments. The chemical composition of carbon steel is given in Table 4.1.

4.3.2 Specification of the insert grades

Tool steel is used as cutting tool for these experiments. Specifications of the cutting tool are given in Table 4.3. This is treated as cantilever beam for these experiments.

4.3.3 Cutting condition

Cutting condition used in machining work pieces is given in Table 4.8. The cutting is in dry state, the presented value was chosen to investigate the effect of superimposed ultrasonic vibration.

Table 4. 8 cutting condition used in experiment

Work piece material	N(rev/min)	D(mm)	V(m/min)	S(mm/rev)	d (mm)
Carbon steel	57	80	14.32296	0.04	0.1
	74	80	18.59472	0.05	0.15
	96	80	24.12288	0.06	0.2

4.4 Results and Discussion

4.4.1 Effect of cutting speed on surface finish

The relation between cutting speed and surface roughness in conventional turning (CT) and ultrasonic assisted turning (UAT) is shown in Figure 4.7 at different feed and depth of cut. The best data collected from a number of tests under the same cutting conditions in both cases are plotted in the graphs. Dashed lines and continuous solid lines show the variation of surface roughness in UAT and CT respectively. In the range of the cutting speeds investigated, the achieved surface roughness of carbon steel work-pieces machined under the application of ultrasonic vibration is superior to the surface roughness of work-pieces machined by conventional cutting. Improvement of surface roughness is about 15-20 % in the

whole range of cutting speeds under investigation. As it is mentioned earlier, when the ultrasonic vibration was applied in the tangential direction the actual surface cutting speed must be well below the critical cutting speed, which is determined by the amplitude and the frequency of the vibrating system. In UAT, because of the effect of pulse cutting force, the width and depth of cutting marks on machined surface are much more uniform.

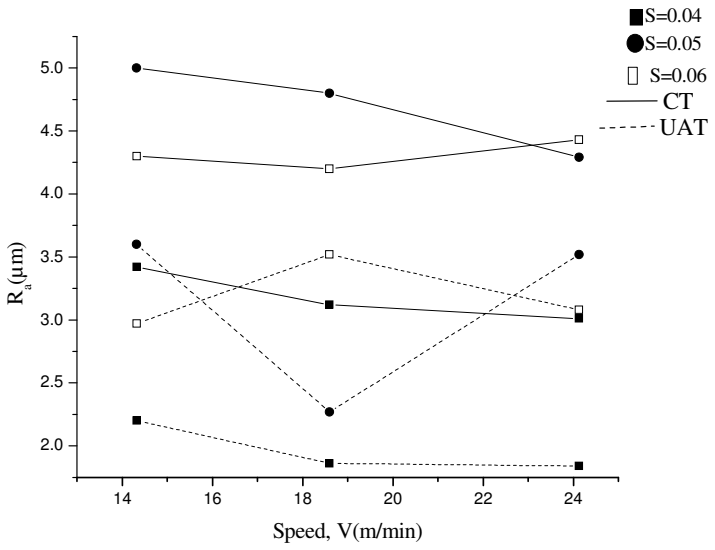

(a)

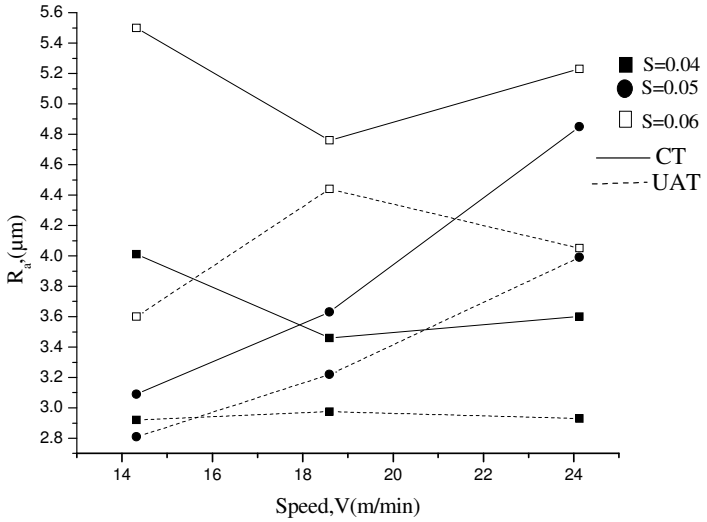

(b)

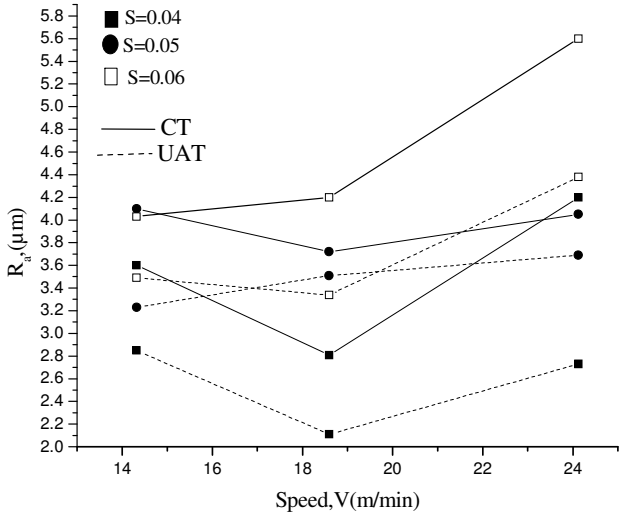

(c)

Figure 4.7 Relative surface roughness(R_a) verses cutting speed(V) (a) depth of cut, d =0.1 (b) d=0.15 (c) d=0.2

During UAT cutting process, it is an intermittent contact between cutter cutting chip and work-piece & cutting chip, so the cooling condition in processing region is better. In addition, at lower cutting speed, curled ribbon chip can produced in ultrasonic turning and the turning process is relatively stable, which is another reason get smaller surface roughness. Low surface roughness in UAT than CT may also be attributed to the fact that built-up-edge formation, the amount of crack and scale are less due to reduced plastic deformation in UAT.

It is also seen that when the cutting speed increases and approaches to critical cutting speed, effect of ultrasonic vibration decreases, the surface roughness increases and approaches to that of CT. It is also observed (indicated in Figs 4.7 a-c) that surface roughness vary due to the resultant effect of cutting speed, feed and depth of cut. This point out that we have to optimizes these parameters to get lowest surface finish under particular working conditions.

4.4.2 Effect of feed on surface finish

The relations between feed rate and surface roughness in CT and UAT are shown in Figure 4.8. Tests results show that surface roughness increases with feed rate, but, it is lower for UAT than CT. Improvement of surface roughness is about 35-40 % in the whole range of feed rates under investigation The reason for this observation lies in that during the CT, the cutting chip will become wider and the vibration in the turning process will become larger with the increase of feed rate, resulting in the enlargement of surface roughness.

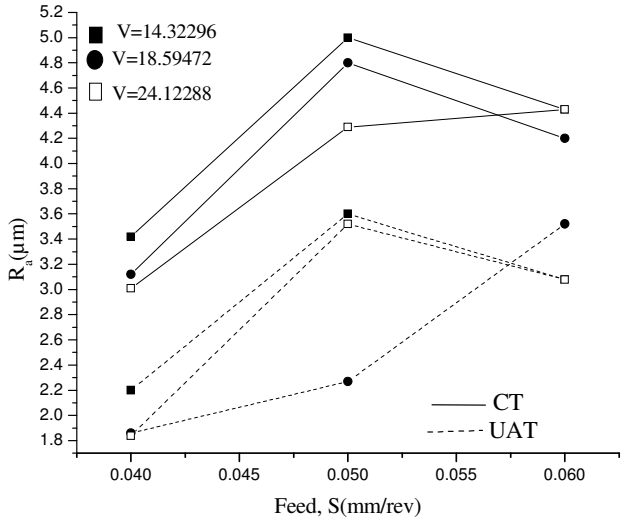

(a)

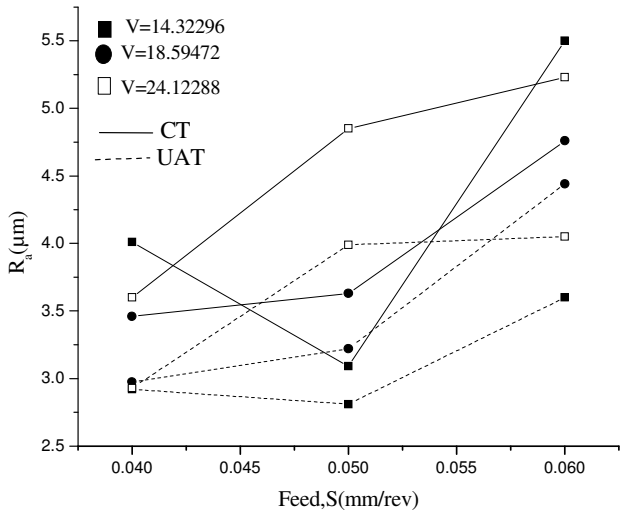

(b)

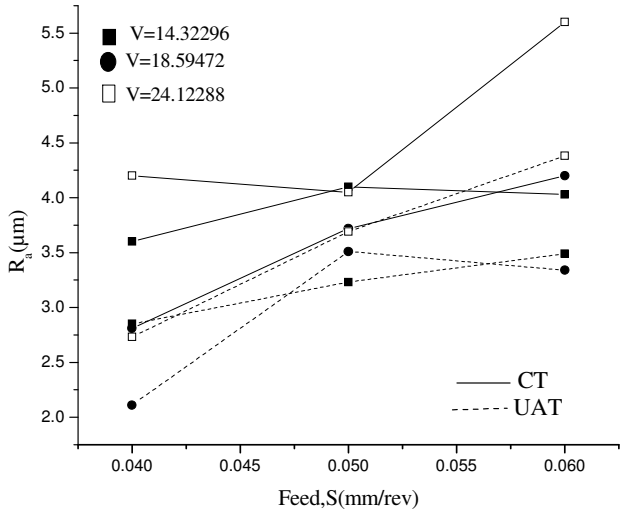

(c)

Figure 4.8 Relative surface roughness (R_a) verses feed (f) (a) depth of cut, d =0.1 (b) d=0.15 (c) d =0.2

While in UAT, the ultrasonic vibration direction is perpendicular to the direction of main cutting force, and the contact between cutter and work-piece is pulse and discontinuous, which is equivalent to reduce the feed rate. So even though under the same cutting conditions, the effect of feed rate in UAT is less than that in CT. A minimum R_a value of

1.8μm was achieved in the test. It is also observed (indicated in Figs 4.8 a-c) that in many cases surface roughness also decreases after reaching a higher value due to the effect of other cutting parameters like cutting speed and depth of cut. It indicates that, it is required to optimize all these parameters to get lowest surface finish under particular working conditions.

4.4.3 Effect of depth of cut on surface finish

Figure 4.9 (a-c) shows the influence of depth of cut on surface roughness. From the figures, it is evident that in the both case of CT and UAT, surface roughness increases with the increase of depth of cut. Although it is lower in case of UAT than CT. Improvement of surface roughness is about 12-18 % in the whole range of cutting speeds under investigation it may be because that cutting force increases with depth of cut, which leads to the increase of vibration in the turning process and the scratches between cutting tool and work piece.

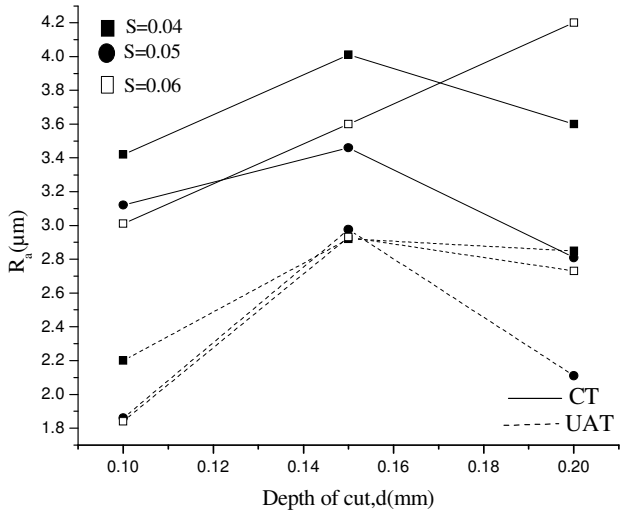

(a)

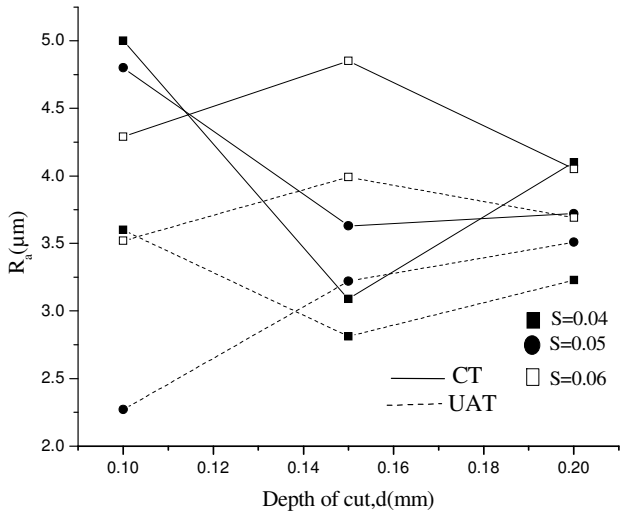

(b)

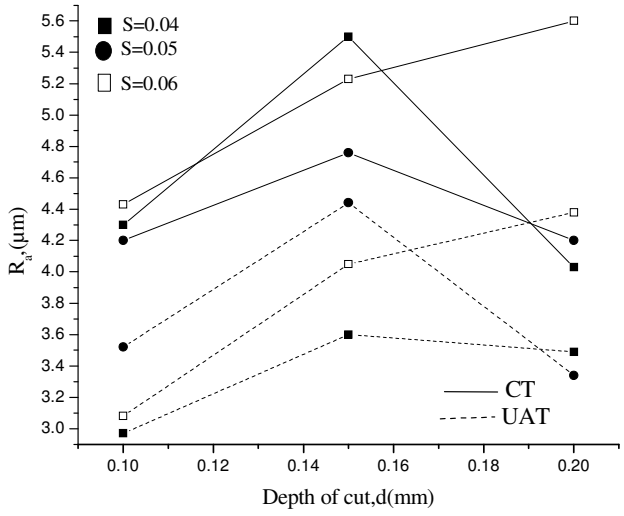

(c)

Figure 4.9 Relative surface roughness (R_a) verses depth of cut (d) (a) speed,V =14.32296 (b) V =1859472 (c) V =24.12288

In UAT decrease in cutting force decline the effect of depth of cut on surface roughness compared with conventional turning. Moreover, during UAT, the increase of cutting depth may reduce the vibration amplitude of the cutting tool; weaken the effect of ultrasonic vibration, which may eventually increase the surface roughness. It is also seen that in many cases surface roughness also decreases after reaching a higher value of depth of cut due to the

effect of overlapping of feed marks influenced by other cutting parameters like cutting speed and feed. It may be due to the minimal difference among the process parameters, limited precision of machine and measuring equipments and interaction among different cutting parameters.

4.4.4 Effect of cutting speed on cutting force

Figures 4.10(a)–(c) sequentially shows the effects of cutting speed on cutting force, namely, average tangential force (F_z) for both the cutting techniques at different feed rate and depth of cut. It can be observed cutting force for the UAT method are reduced up to 25–35% that is required for the CT method at all the cutting speeds. As explained earlier, it is due to the fact that UAT gives rise to intermittent contact between cutting tool tip and chip and work-piece & cutting chip, so better cooling condition in processing region. In addition, UAT promotes curled ribbon chip, relatively stable turning process, lessen formation of built-up-edge formation due to reduced plastic deformation.

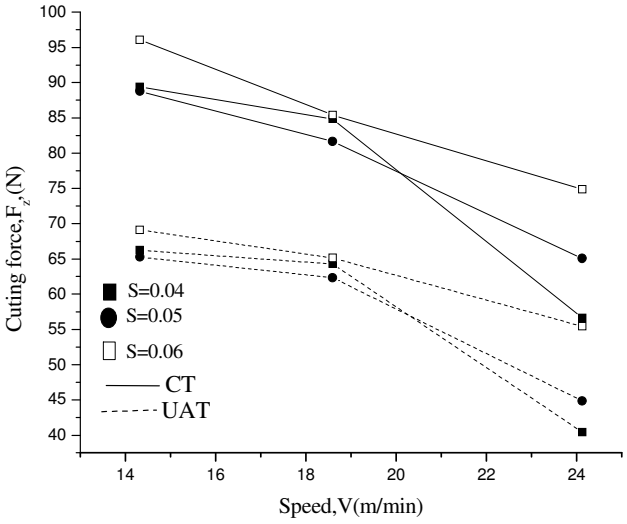

(a)

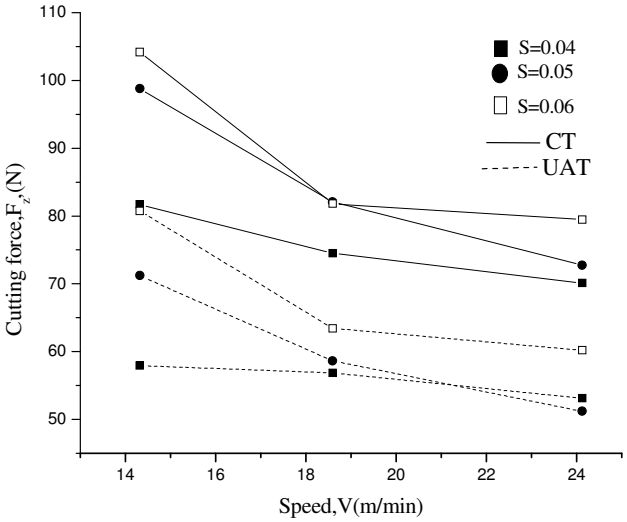

(b)

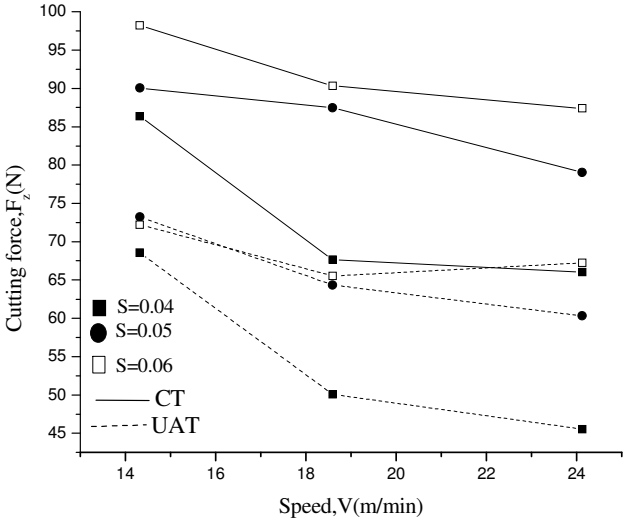

(c)

Figure 4.10 Principal cutting force (F_z) verses speed (V) (a) depth of cut, d =0.1 (b) d=0.15 (c) d=0.2

It can be noticed that the tangential force values decrease with the increase in spindle speed (or nominal cutting speed). Two reasons can be realized with this observation. One reason is that larger shear angle and thus a smaller resultant average force value is induced by the increased speed. Another reason is that an increased speed ratio, which is linearly related with

nominal cutting speed, leads to more overlapping cutting cycle and hence a relatively smaller thickness of cut. This smaller thickness of cut decreases the material load on the tool rake face eventually lead to a smaller cutting force.

4.4.5 Effect of feed on cutting force

In Figures 4.11 (a-c), the cutting force in most of the cases increases insignificantly with the increase in feed rate in UAT, like the variation trend in the CT method. However, cutting force, at almost all the feed rates, in the UAT process are reduced approximately to about 25–30% of that of the CT process. Such phenomenon is deemed to be caused by the increase in uncut chip thickness induced by the increment in feed rate. Due to the bigger uncut chip thickness, more cutting area leads to increase of cutting force.

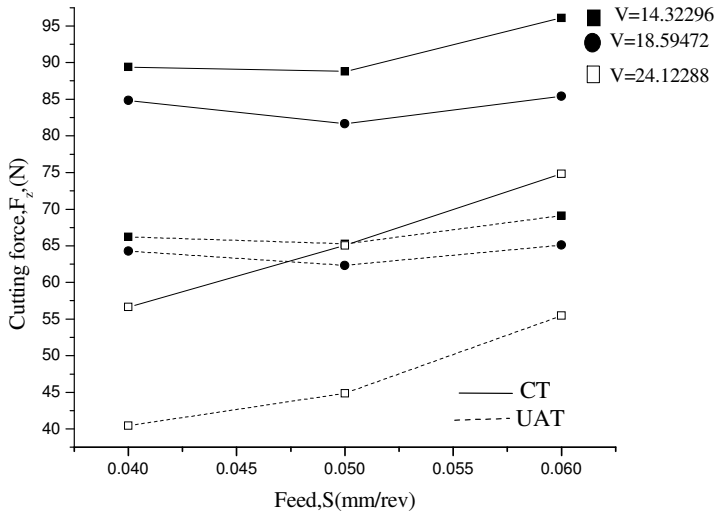

(a)

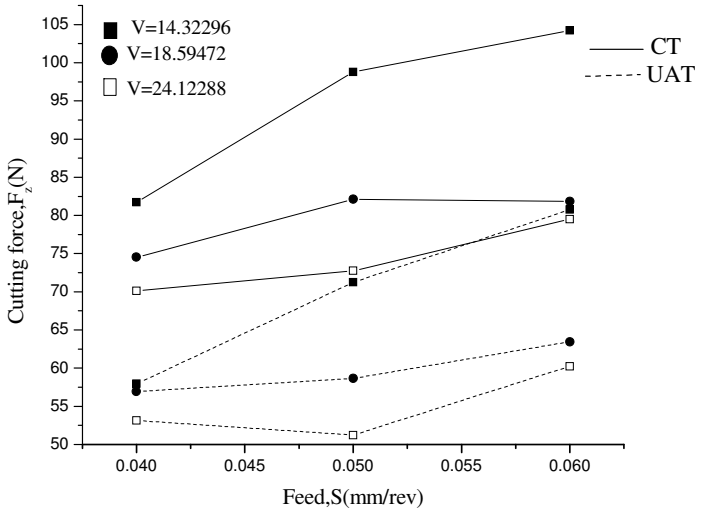

(b)

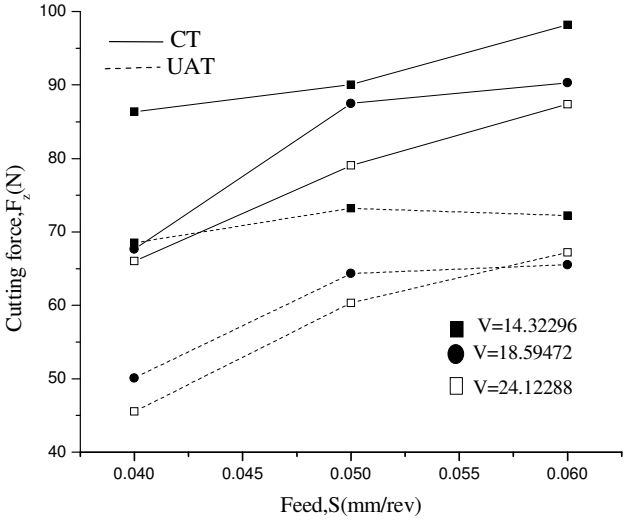

(c)

Figure 4.11 Principal cutting force (F_z) verses feed (f) (a) depth of cut, d =0.1 (b) d=0.15 (c) d=0.2

4.4.6 Effect of depth of cut on cutting force

Similarly, Figures 4.12(a)-(c) show that the tangential cutting force values, barring at higher feed (0.06 mm/rev) and higher depth of cut (0.15-0.2 mm), in most of the cases increase with

the increase in depth of cut in the UAT method, similar to the observation in the CT process, due to increased pressure on the tool rake face. However, cutting force, at almost all the depth of cuts, in the UAT process are reduced approximately to about 20–25% of that of CT process. It is also seen that in some cases cutting force decreases after reaching a higher value due to the effect of other cutting parameters like cutting speed and feed. It signifies that, optimization of all the cutting parameters is essential to get minimum cutting force at a particular working condition.

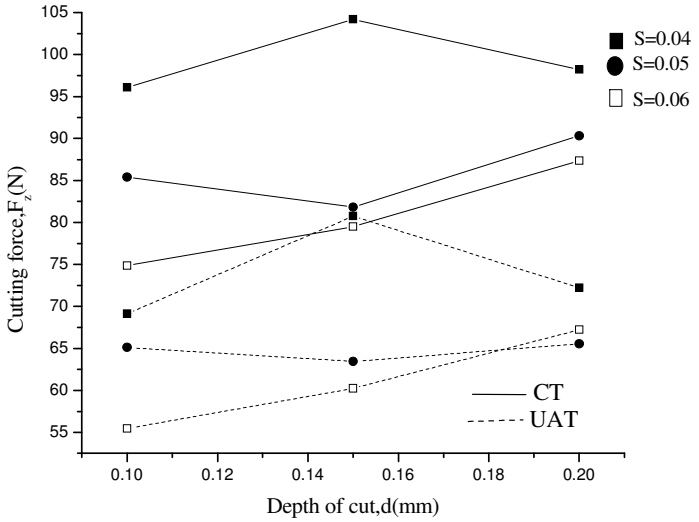

(a)

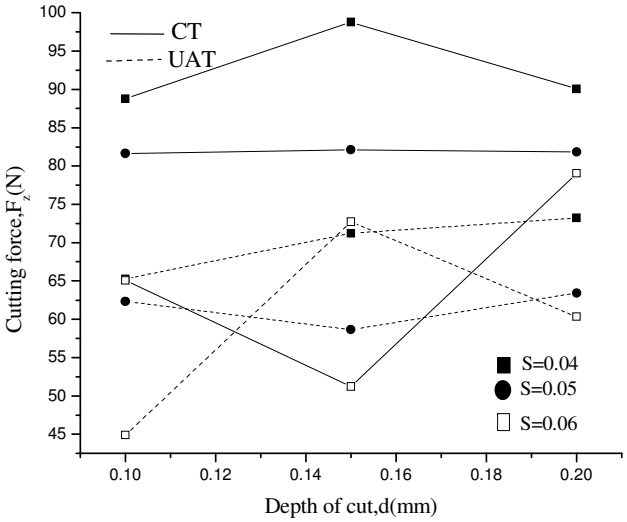

(b)

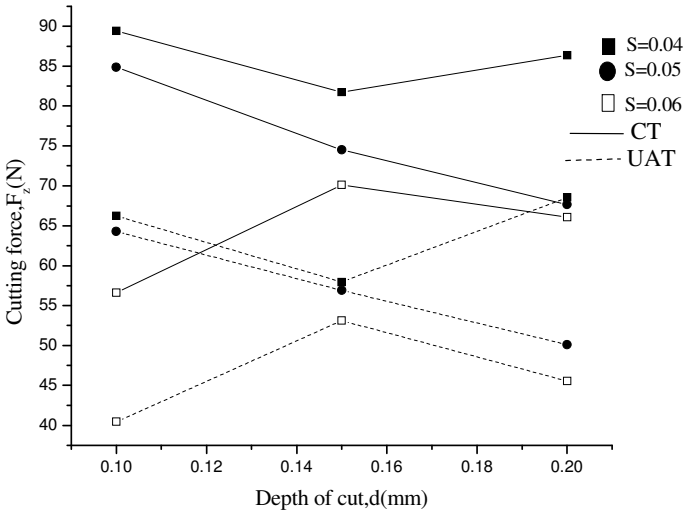

(c)

Figure 4.12 principal cutting force (F_z) verses depth of cut (d) (a) speed, V = 24.12288 (b) V =18.59472 (c) V =14.32296

4.5 Conclusions

The following conclusions can be drawn based on the results of the experimental study on turning carbon steel by conventional turning (CT) and ultrasonic assisted turning (UAT).

In UAT, feed rate has considerable influence on surface roughness while the influence of depth of cut and cutting speed on surface roughness become less intense than others

parameters. UAT improved the surface roughness by 12.0–40.0%. It proves that UAT can obtain smoother surface.

Because of the unstable turning process in CT, the surface can easily produce some defects such as burrs, tearing and so on, so the quality of surface becomes poor. While the UAT can reduce the influence of deformation and built-up-edge formation because of high frequency reciprocating movement between the contacting surfaces of the tool and the work piece, so as to make the turning process more stable.

The test results show that the cutting force for the UAT method decreases by 25.0–35.0 % in comparison with CT. As a result, ultrasonic-aided cutting can enhance the cutting quality of carbon steel.

Chapter-5

Optimization of UAT parameters

CHAPTER 5

OPTIMIZATION OF UAT PARAMETERS

5.1 Design of Experiment

In the present work experiments are done according to design of experiment [47] and the data analyses are made with application of design of experiment (DOE) techniques and response surface methodology in developing mathematical model relating important input variables i.e. cutting speed, feed, depth cut, surface roughness and principal cutting force. All these statistical analysis are done by commercial available software Minitab 15®[48].

Objectives:

- To use response surface methodology in developing mathematical model relating important input variables and responses.
- Adapting L_9 orthogonal array to the design of experiment .The experimental design has 3 levels and 3 factors.
- Optimize Process parameters using Grey-based Taguchi method.

5.1.1 Full factorial design

In full factorial experiment, responses are measured at all combinations of the experimental factor levels. The combinations of factor levels represent the conditions at which responses will be measured. Each experimental condition is a called a "run" and the response measurement an observation. The entire set of runs is the “design”.

5.1.2 ANOVA

ANOVA (analysis of variance) is a method of computation to identify the differences between two or more sovereign groups of data collected. Source of variation are explained in their degree of freedom (DF), total sum of square (SS), and the mean square (MS). The analysis will calculate also the F-statistic and p-values which are to determine whether the predictor of factors is significant or insignificant related to the response (The detail calculations are provided in Appendix A).

5.1.3 Response surface methodology (RSM)

Response Surface Methodology is one of the useful tools in statistical analysis used to examine the relationship between one or more response variables and a set of quantitative experimental variables. It is common in industries that when the data are not manageable and

unstructured leads to a brunt in waste of energy and correctness of components. RSM is a technique of identifying the handy and disobedient data to find the optimum performance and optimize the response.

In the present analysis a central composite matrix is used in order to optimize the experimental conditions of surface texturing process. Central composite second order design is found to be the most efficient tool in response surface modeling using the smallest possible number of tests that still guaranteed a good accuracy. The Mathematical model of Response surface methodology (RSM) model corresponds to a second-order polynomial expressed by (Eq 5.1)

$$\ddot{Y} = b_0 + \sum_{i=1}^{n} b_i x_i + \sum_{i=1}^{n} b_{ii} x^2_i + \sum_{\substack{i,j=1 \\ i \neq j}}^{n} b_{ij} x_i x_j \qquad (5.1)$$

Where $\ddot{Y}$ is the corresponding objective function, X_i the coded values of the i_{th} influencing factor, n the numbers of factors and b_0, b_i, b_{ii}, b_{ij}, are the regression coefficients.

5.1.4 Taguchi method

This is a statistical experimental design to calculate a single or multiple groups of data (variable) to find the optimum and steadiness in the operating surroundings (response). It also can distinguish the convenient and uncontainable factors in order to minimize the effect of noise factors. Taguchi design is used in an orthogonal array which can estimate the effect of each factor relative to the means and variation. The orthogonal array design is for investigating the effect of each factor independently from the other in an economic way which reduces time and cost efficiently. The main objective is to identify the factors that affect the mean response and control them into the optimum level.

Herein we deal with the analysis of the experiment by the Taguchi methodology, which consists of the orthogonal arrays. L_9 orthogonal arrays have been used to determine the importance of the factors or the parameters. For the experimental work our main responses are: Surface roughness (R_a) and Principal cutting force (F_z)

5.1.5 Calculation of Grey relational grade

Taguchi method alone cannot solve multi-objective problems. Grey relational analysis is used to convert a multi-objective problem into a single objective problem. In Grey relational analysis firstly the experimental data i.e., measured quantity characteristics are normalized ranging from zero to one. This process is called as Grey relational generation. Depending upon the criteria objective function may be Lower-the-Better, Higher-the-Better or Nominal-is-Best.

Step-1: Grey relation generation

For Lower-the-Better

$$Xi(k) = \frac{\max Yi(k) - Yi(k)}{\max Yi(k) - \min Yi(k)} \tag{5.2}$$

For Higher-the-Better

$$Xi(k) = \frac{Yi(k) - \min Yi(k)}{\max Yi(k) - \min Yi(k)} \tag{5.3}$$

Where $X_i(k)$= Value after Grey relational generation

Min $Y_i(k)$= minimum of Yi(k) for K_{th} Response

Max $Y_i(k)$= maximum of Yi(k) for k_{th} Response

Step-2: Calculation of Grey relation co-efficient

$$\Psi i(k) = \frac{\Delta \min + \Psi \Delta \max}{\Delta 0i(k) + \Psi \Delta \max} \tag{5.4}$$

Where $\Delta_{0i(k)} = |x_{0(k)} - x_{i(k)}|$ = Difference between absolute Values of $x_{0(k)}$ and $x_{i(k)}$

Step-3: After taking average of the Grey relational coefficients, the Grey relational grade (γ_i) can be calculated

$$\gamma_i = \sum_{k=1}^{n} \xi_i(k) \tag{5.5}$$

5.2 Results and Discussion

5.2.1 Development of model based on RSM

Table 5.1 Experimental factor and their levels

Process parameter	Level-1	Level-2	Level-3
Depth of cut (d)	0.1 mm	0.15 mm	0.2 mm
Feed(S)	0.04mm/rev	0.05mm/rev	0.06 mm/rev
Speed(V)	14.323 m/min	19.223 m/min	24.122 m/min
Amplitude	16 µm		
Frequency	20kHz		

Table 5.2 Response surface design (UAT)

Run	d	S	V	R_a(μm)	F_z(N)
1	-1	-1	-1	2.200	66.22
2	1	1	-1	3.490	72.22
3	1	-1	1	2.730	45.55
4	-1	0	1	1.864	55.44
5	0	0	0	2.270	58.66
6	0	0	0	2.260	57.66
7	1	-1	-1	2.850	68.54
8	-1	1	-1	2.970	69.12
9	-1	-1	1	3.490	40.45
10	1	1	1	4.707	67.22
11	0	0	0	3.220	57.66
12	0	0	0	3.000	62.33
13	-1	0	0	2.270	61.22
14	1	0	0	3.510	64.33
15	0	-1	0	2.410	56.89
16	0	-1	0	4.440	63.44
17	0	0	-1	2.810	71.22
18	0	0	1	3.990	51.22
19	0	0	0	3.220	58.62
20	0	0	0	3.110	58.83

After knowing the values of the observed response, the values of the different regression coefficients of second order polynomial mathematical equation i.e. Eq.5.1 has been evaluated and the mathematical models based on the response surface methodology have been developed by utilizing test results of different responses obtained through the entire set of experiments.

5.2.1.1 Model of surface roughness

The response surface methodology based analysis has been done to establish the mathematical model through the development of mathematical relationship between surface roughness and the important process parameters, as feed(S), speed (V) and depth of cut (d). Based on the roughness test results obtained from the planned experiments, as shown in Tables 5.1 and 5.2, the values of the different constants of the Eq. 5.1 are obtained for surface roughness model. The mathematical relationship for correlating the roughness, i.e., R_a phenomenon and the considered machining parameters has been established as follows:

$$R_a = 16.5532 - 4.6257d - 541.0984S - 0.1841V - 129.1843d^2 + 4950.3992S^2 + 0.078V^2 + 868.25d*S + 0.4685d*V - 2.7016S*V$$

R-Sq=92.0%, R-Sq (adj) =81.1%

5.2.1.2 Model of principal cutting force

Based on Eq. 5.1, the effects of various machining process variables, e.g. depth of cut (d), feed(S) and speed (V) on principal cutting force (F_z) has been evaluated by computing the values of different constants of Eq. 5.1 utilizing the relevant experimental data from Table 5.2. The mathematical relationship for correlating the average principal cutting force and the considered machining process parameters is obtained as follows:

$$F_z = 165.0085 - 369.026d - 431.9322S - 6.8666V + 714.000d^2 - 8250.000S^2 + 0.0096V^2 + 1865.000dS + 5.8470dV + 76.7355SV$$

R-Sq=96.2%, R-Sq (adj) =92.8%

5.2.1.3 Adequacy test for surface roughness and principal cutting force

An ANOVA table is generally used to check the adequacy of the model developed. Depending upon F-value (variance ratio), p-value (probability of significance) is calculated. If p value of model is less than 0.05, significance of corresponding term is established and is desirable as it indicates that the terms in the model have a significant effect on the response. From ANOVA Tables 5.3 and 5.4, analyzing of variance shows that the regression model is significant as the values of probability less than 0.05. The model proposed is statistically significant and adequate because of high R^2 value. The co-efficient of determination is more than 80% for the above model developed, which shows the high co-relation, existing between the experimental and predicted values. The adjusted R^2 value is particularly useful when comparing models with different number of terms. When the R^2 approaches to unity, the better the response model fits the actual data.

In surface response model, the adjusted R^2 (81.1) is closed to the predicted R^2 (92.0) and in principal cutting force model, the adjusted R^2 (92.8) is closed to the predicted R^2 (96.2). So the predicted R^2 is in reasonable agreement with the adjusted R^2. It is understood that unnecessary terms are not added in the model. The model presented high determination coefficient (R^2=92.0 & 96.2 close to unity) explaining 92.05% & 96.2% of variability in the response which indicates the goodness of fit for the model & high significance of the model. This analysis shows that the prediction model sufficiently explains the relationship between the responses and independent variables.

Table 5.3 ANOVA for R_a (RSM model)

Source	DF	Seq SS	Adj SS	Adj MS	F	p
Regression	9	6.4646	6.46464	0.71829	6.95	0.006
Linear	3	3.6644	3.66442	1.22147	11.82	0.003
Square	3	1.0481	1.04813	0.34938	3.38	0.075*
Interaction	3	1.7521	1.75210	0.58403	5.65	0.022
Residual Error	8	0.8269	0.82690	0.10336		
Total	19	10.3988				
*= insignificant factor						

Table 5.4 ANOVA for F_z (RSM model)

Source	DF	Seq SS	Adj SS	Adj MS	F	p
Regression	9	1225.61	1225.61	136.179	28.36	0.000
Linear	3	1077.05	1077.05	359.016	74.76	0.000
Square	3	12.09	12.09	4.029	0.84	0.503*
Interaction	3	136.47	136.47	45.491	9.47	0.003
Residual Error	10	48.02	48.02	4.802		
Total	19	1273.63				
*= insignificant factor						

5.2.3 Parametric optimization

Table 5.5 Experimental result of Taguchi L_9 orthogonal array

Run	D	S	V	R_a	F_z
1	1	1	1	2.2	66.22
2	1	2	2	2.27	62.33
3	1	3	3	3.08	55.44
4	2	1	2	2.41	56.89
5	2	2	3	3.13	51.22
6	2	3	1	3.6	80.77
7	3	1	3	2.73	45.55
8	3	2	1	3.23	73.22
9	3	3	2	3.34	65.55

5.2.3.1 Influence on surface roughness

During the process of UAT, the effects of various machining parameters like d, S, V on R_a are shown in Figure 5.1.This figure indicates that the effect of depth of cut on surface finish is more as compared to speed and feed. So the percentage of contribution according to ANOVA Table 5.6 of depth of cut, feed and speed are 55.76, 29.41, and 9.17 respectively.

From the present analysis it is found that all factors are insignificant and the percentage of contribution of depth of cut for surface finish in UAT is more and followed by feed and speed.

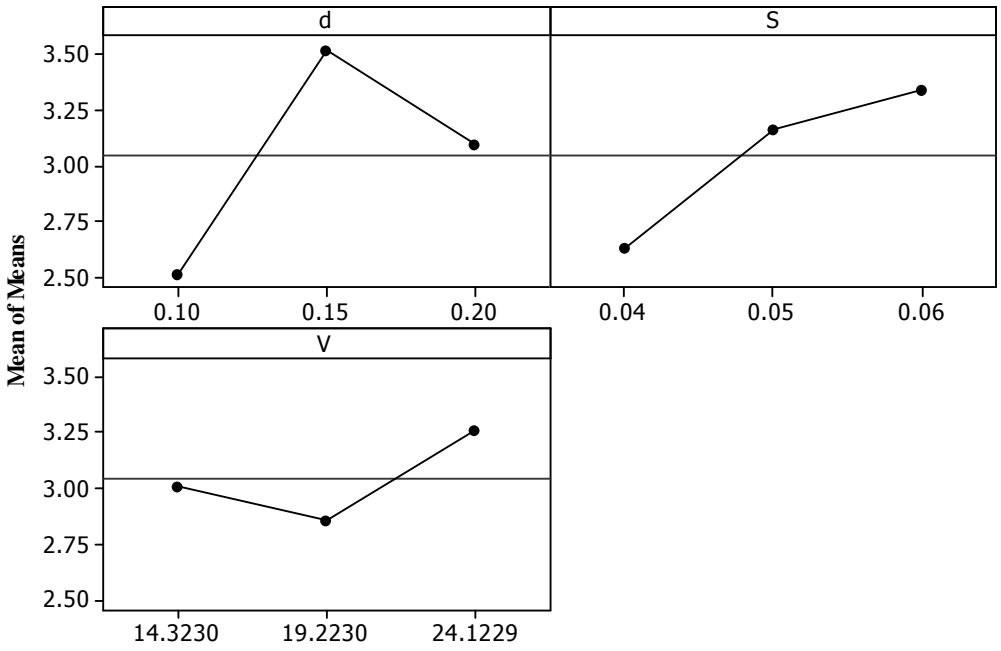

Figure 5.1 Main effect plots for R_a

Table 5.6 ANOVA for R_a (Taguchi)

Source	DF	SS	MS	F	p	%contribution
d	2	1.5291	0.76453	9.86	0.092*	55.76
S	2	0.8066	0.40328	5.20	0.161*	29.41
V	2	0.2515	0.12577	1.62	0.381*	9.17
Error	2	0.1550	0.07750			5.65
Total	8	2.7421				100
*=insignificant						

5.2.3.2 Influence on principal cutting force

Influence on F_z is shown in Figure 5.2 indicates that effects of speed is more as compared to feed and depth of cut. From ANOVA, Table 5.7, it is shown that both speed and feed are significant factors at 95% confidence level and percentage of contribution of speed, feed and depth of cut are 79.94,18.98,.05 respectively.

Table 5.7 ANOVA for F_z (Taguchi)

Source	DF	SS	MS	F	p	%Contribution
d	2	4.979	2.490	0.93	0.518*	0.05
S	2	183.142	91.571	34.20	0.028	18.98
V	2	771.127	385.564	143.91	0.007	79.94
Error	2	5.355	2.678			0.055
Total	8	964.605				100
*=insignificant factor						

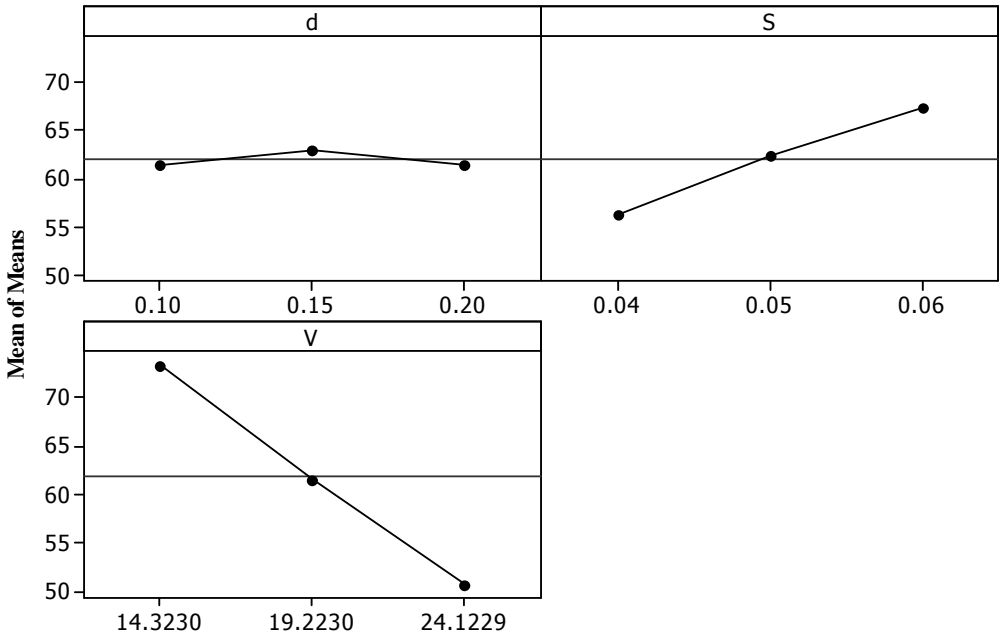

Figure 5.2 Main effect plots for F_z

5.2.3.3 Optimization by Grey relation analysis

In the present Grey relation analyses, optimal parametric combination for surface roughness & principal cutting force (multi objective) of UAT has been evaluated. The Grey relation grade and rank is shown in Table 5.8 and Figure 5.3. Thus, the multi criteria optimization problem has been transferred into a single equivalent objective function optimization problem using the combination of the Taguchi approach and grey relation analyses. The higher the value of the grey relation grade, the corresponding factor combination is said be close to the optimal. The mean of the grey relation grade for each level of cutting parameters, and the total mean of the grey relation grade is summarized in Table 5.9. Figure 5.4 shows that the grey relation grade (GRG) graph and is represented graphically in main effect plot. With the help of mean grey relation grade, the optimal parametric combination becomes d_3-S_1-V_3 &

from mean effective for GRG graph the optimal parametric combination become d_1-S_1-V_3. The significance of the factors on the overall quality characteristics of ultrasonic assisted turning (UAT) process has also been evaluated quantitatively with the analysis of variance (ANOVA) method for grey relation grade and shown in Table 5.10. Results of ANOVA indicate that feed is the most significant factor followed by cutting speed as the p-values is less than 0.05. Cutting speed and depth of cut are found to be insignificant from the study. Optimal results were verified through confirmation test. Table 5.11 shows the comparison of the estimated grey relation grade with the actual grey relation experiments using optimal cutting parameters. It may be noted that there is good agreement between the estimated value 0.784553 and experimental value 0.810078. The improvement of grey relation grade from initial parameter is 0.476748.

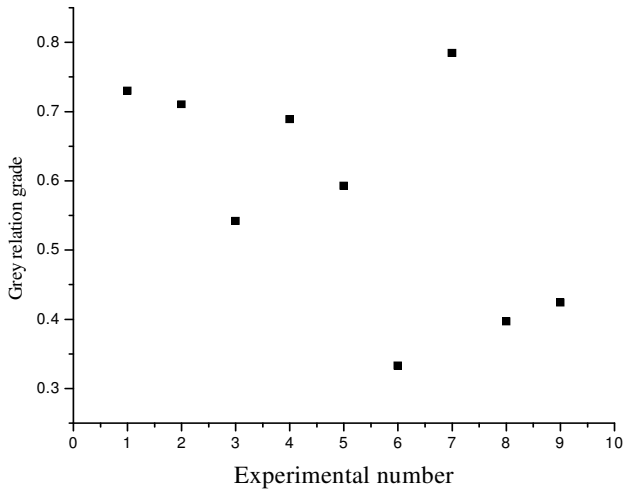

Figure 5.3 Grey relation grade

Table 5.8 Grey relation analysis table

Run	R_a	F_z	Normalizing		GRC		GRG(γ)	Ranking
			R_a	F_z	R_a	F_z		
1	2.2	66.22	1	0.413118	1	0.460031	0.730016	2
2	2.27	62.33	0.95	0.523566	0.909091	0.512067	0.710579	3
3	3.08	55.44	0.371429	0.719194	0.443038	0.640364	0.541701	6
4	2.41	56.89	0.85	0.678024	0.769231	0.60829	0.68876	4
5	3.13	51.22	0.335714	0.839012	0.429448	0.756443	0.592946	5
6	3.6	80.77	0	0	0.333333	0.333333	0.333333	9
7	**2.73**	**45.55**	**0.621429**	**1**	**0.569106**	**1**	**0.784553**	**1**
8	3.23	73.22	0.264286	0.214367	0.404624	0.388913	0.396769	8
9	3.34	65.55	0.185714	0.432141	0.380435	0.468227	0.424331	7

Table 5.9 Response table for GRG

UAT Parameter	Average GRG by Factor Level			Max-Min
	Level 1	Level 2	Level 3	
d	0.6608	0.5383	0.5352	0.1255
S	0.7344	0.5668	0.4331	0.3031
V	0.4867	0.6079	0.6397	0.1530
Total mean relation grade=0.57811				

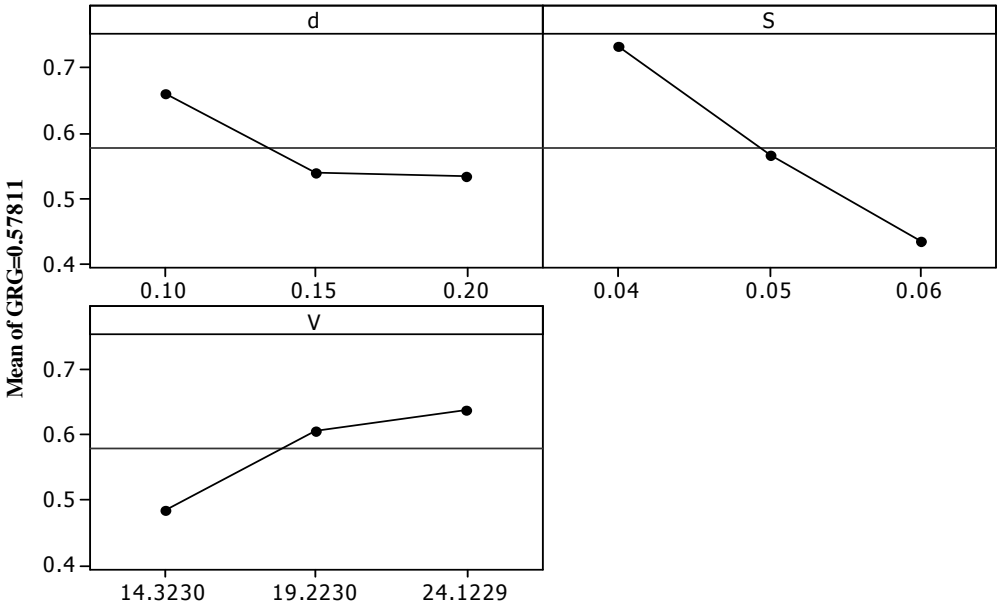

Figure 5.4 Effect of UAT parameter level on the multi performance

Table 5.10 ANOVA for grey relation grade

Source	DF	SS	MS	F	p	%Contribution
d	2	0.030758	0.030758	4.50	0.182*	14.38
S	2	0.136771	0.136771	2.02	0.048	63.95
V	2	0.039117	0.039117	5.72	0.149*	18.29
Error	2	0.006833	0.006833			3.19
Total	8	0.213840				100
*=insignificant factor						

Table 5.11 Results of confirmatory experiment

	Initial factor setting	Optimal cutting factors	
		Prediction by GRG	Experimental(Figure 5.4)
Level	d_2-S_3-V_1	d_3-S_1-V_3	d_1-S_1-V_3
R_a	3.6		2.8
F_z	80.77		44.22
GRG(γ)	0.333333	0.784553	0.810078
Improvement in grey relation grade=0.476748			

5.4 Conclusions

In this study, response surface methodology for the optimization of machining parameters is proposed. Statistical models have been developed for the cutting force (F_z) and surface roughness (R_a) using central composite design with three level factors. Mathematical models' output revealed that the RSM model proposed are statistically significant and adequate for all the environmental conditions because of higher R^2 value (0.92 and 0.962), which is close to 1. It shows the high correlation exist between the experimental and predicted values.

Optimization of multiple performance characteristics of the UAT such as surface roughness and cutting force has been carried out using Taguchi-based GRA technique. The factors considered for the L_9 orthogonal array construction are the cutting speed, feed, and depth of cut. The contribution of each factor towards the multi-response optimization has been studied and it is inferred that combining Taguchi method and GRA are well applicable for the optimal design of UAT.

Further the developed models from multiple response optimizations, the optimum machining conditions for the spindle speed, feed rate and depth of cut are determined as, 24.122 m/min, 0.04mm/rev and 0.1mm respectively. The optimized machining parameters are used for the confirmation of experiments for validation and it is observed that the improvement of grey relation grade from initial parameter is 0.476748, showing good agreement with the predicted responses.

Chapter-6

Conclusions and Future Recommendations

CHAPTER 6

CONCLUSIONS AND FUTURE RECOMMENDATIONS

6.1 Conclusions

In this work the influence of cutting parameters (cutting speed, feed and depth of cut) on UAT cutting force and surface roughness acting on carbon steel has been investigated. The results have been compared with those obtainable from the conventional turning process. The influencing parameters of the horn design have also been investigated. The following conclusions could be drawn from this investigation:

- In UAT, feed rate has considerable influence on surface roughness while the influence of depth of cut and cutting speed on surface roughness become less intense than others parameters. UAT improved the surface roughness by 12.0–40.0%. The test results show that the cutting force for the UAT method decreases by 25.0–35.0 % in comparison with CT.

- Modal analysis of the cutting tool is performed. During the analysis of frequency response characteristics it is found out, that dominant peaks correspond the respective modes. Dominant peaks are in longitudinal direction at approximately 19.5 kHz excitation frequency. According to modal analysis the 2^{nd} mode is at excitation frequency 22.7 kHz. Here the cutting tool is vibrating in longitudinal direction. After this analysis the conclusion can be made, that: for exiting longitudinal vibrations and vibrations in cutting direction is purposeful to excite in 1^{st} mode of the cutting tool.

- The present study develops roughness and cutting force models for three different cutting parameters using response surface method. The second-order response models have been validated with analysis of variance. It is found that all the three cutting parameters (spindle speed, depth of cut and feed rate) and their interactions have significant effect on roughness parameters considered in the present study though the influences may vary with the nature of work-piece material. An attempt has been made to estimate the optimum cutting conditions to produce the best possible surface quality and lowest cutting force requirement separately within the experimental

constraints. Optimum machining parameter combinations for different roughness parameters are also tested through confirmation experiments that show fairly good agreement with prediction of response surface method.

- UAT process has several performance measures (responses) and some of these responses are correlated. Reported researches in the literature on UAT processes mainly deal with the optimization of single performance measure at a time. In this work, GRA method which can be effectively used to optimize multiple correlated responses of UAT process is presented. Using this method, two sets of past experimental data on UAT process are analysed and the optimization performance found out.

- To conclude, the UAT method has been found to be a suitable technique to achieve high-quality finish surfaces and lower cutting force requirement not only for hard material but also for general purpose engineering material, like carbon steel.

6.2 Future Recommendations

- Further investigation is necessary to assess the impact of cutting tool edge condition, effect of rake angle and effect of the process on various materials.
- More study is essential to know the effect of vibration parameters amplitude, frequency, direction of vibration on cutting performance, location of the UAT on the tool.
- Further analysis is required to find out the tool life, residual stress and temperature rise in UAT method
- The same experiment needs to be carried out at least more than 3 times for its repeatability and error bar can be plotted.
- The sensitivity analysis for the FE mesh needs to be done.
- In the FE analysis, the elastic deformation of the vibrating tool and stress distribution may be included to get better result.

REFERENCES

REFERENCES

[1] Shamato, E.C., X. Ma and T. Morowaki, "Ultraprecision ductile cutting of glass by applying ultrasonic elliptical vibration cutting", *Precision Engineering Nanotechnology*, 1, 1999, pp 408-411.

[2] Markov, A. I., "Ultrasonic machining of intractable materials", 1996, London: Iliffe Books Ltd.

[3] Kumabe, J., "Vibratory cutting", 1979, Dzikke Sjuppan, Tokyo.

[4] Devin, J., "Ultrasonically assisted metal removal", *SAMPLE Quarterly*, 10, 1979, pp 485-496.

[5] Takeyama, H. and Iijima, "Machinability of glass fiber reinforced plastics and application of ultrasonic machining", *Annals CIRP*, 37(1), 1988, pp 93-96.

[6] Kremer, D., "Ultrasonically assisted machining", *Mech. Ind. Mater*., 48, 1995, pp.15-21.

[7] Astashev, V.K., "Effect of ultrasonic vibrations of a single point tool on the process of cutting", *Journal of Machinery Manufacturing and Reliability*, 5, 1992, pp 65–70.

[8] Morowaki, T., E., Shamoto and K. Inoue, "Ultra precision ductile cutting of glass by applying ultrasonic vibration", *CIRP Annals*, 41, 1992, pp 559-562.

[9] Astashev, V. K., and V. I. Babitsky, "Ultrasonic cutting as a nonlinear (vibro-impact) process", *Ultrasonics*, 36, 1998, pp 89-96.

[10] Babitsky, V.I., A. N. Kalashnikov, and A. Meadows, "Ultrasonically assisted turning of aviation materials", *Journal of Materials Processing Technology*, 132, 2003, pp 157-167.

[11] Masahiko, Jin, Masao Murakawa, "Development of a practical ultrasonic vibration cutting tool system". *Journal of Materials Processing Technology*, 113, 2001, pp 342-347

[12] Isaev, A. and V. Anochin, *Vestnik Mashinostroenia,* 5, 1961, pp 56.

[13] Kubota, M., J. Tamura and N. Shimamura, *Bull. Jap.Soc.Proc.Engng*, 11, 1977, pp.127.

[14] Markov, A.I., "Ultrasonic Machining of Hard Materials", 2nd ed.1968, Moscow: Machinostroenie.

[15] Kim, J.D. and E.S. Lee, "A study of ultrasonic vibration cutting of carbon fiber reinforced plastics", *International Journal of Advance Manufacturing Technology*, 12, 1996, pp 78-86.

[16] Weber, H., J.Heberger and R. Plitz, "Turning of machinable glass ceramics with an ultrasonically vibrated tool", *Annals of the CIRP*, 33, 1984, pp 85-87.

[17] Kim, J.D. and I.H.Choi, "Micro surface phenomenon of ductile cutting in the ultrasonic vibration cutting of optical plastics", *Journal of Materials Processing Technology*, 68, 1997, pp 89-98.

[18] Klocke, F. and O.Rubenach, "Ultrasonic–assisted diamond turning of glass and steel", *Industrial Diamond Review*. 60, 2000, pp 227-239.

[19] Skelton, R.C., "Effect of ultrasonic vibration on the turning process", *International Journal of Machine Tool Design and Research*, 9, 1969, pp. 363-374.

[20] Zhong, Z.W. and G. Lin, "Diamond Turning of a Metal Matrix Composite with Ultrasonic Vibrations". *Materials and Manufacturing Processes*, 20, 2005, pp 727-735.

[21] Zhong, Z.W. and G. Lin, "Ultrasonic assisted turning of an aluminium-based metal matrix composite reinforced with SiC particles". *The International Journal of Advanced Manufacturing Technology,* 27, 2005, pp 1077-1081.

[22] Liu, K., X.P. Li, and M. Rahman, "Characteristics of ultrasonic vibration-assisted ductile mode cutting of tungsten carbide". *The International Journal of Advanced Manufacturing Technology,* 35, 2008, pp 833-841.

[23] Chen, J., G.Tian, Y.Chi, M.Liu, D.Shan and Y.Liu, "Surface Roughness and Microstructure in Ultrasonically Assisted Turning of W-Fe-Ni Alloy", *Journal of Materials Processing Technology*, 199, 2008, pp 441-444.

[24] Hsu, C., Y. Lin, W. Lee, and S. Lo, "Machining characteristics of Inconel 718 using ultrasonic and high temperature-aided cutting", *Journal of Materials Processing Technology*, 198, 2008, pp 359-365.

[25] Nath, C., and M. Rahman, "Effect of machining parameters in ultrasonic vibration cutting", *International Journal of Machine Tools and Manufacture*, 48, 2008, pp 965-974.

[26] Jiao, F., X. Liu, C.Y. Zhao, and X. Zhang, "Experimental Study on the Surface Micro-Geometrical Characteristics of Quenched Steel in Ultrasonic Assisted Turning", *Advanced Materials Research*, 189, 2011, pp 4059-4063.

[27] Cheng X. and X.Ma, "Microstructure Analysis of SiCp / Al Composites with Ultrasonic Vibration Turning", *International Conference on Biomedical Engineering and Informatics*, 3, 2010, pp 2321-2324.

[28] Childs, T., K.Maekawa, T.Obikawa, and Y.Yamane, "Metal machining theory and application", Arnold, London,2000.

[29] Trent, E. and P.Wright, "Metal cutting", Butterworth-Heinemann, London, 2000.

[30] Ceretti, E.,M.Lucchi and T.Alan "FEM simulation of orthogonal cutting; serrated chip formation", *Journal of Materials Processing Technology*, 95, 1999, pp 95-99.

[31] Anagonye, A. and D. Stephenson, "Modelling cutting temperature for turning inserts with various tool geometries and materials", *Transaction. ASME. Journal of Manufacturing Science and Engineering* , 124, 2002, pp 78-85.

[32] Pantale, O., J.L.Bacaria, O.Dalverny, R.Rakotomalala and S.Capera "2D and 3D numerical models of metal cutting with damage effects", *Computational method for Applied Mechanical Engineering,* 193, 2004, pp 134-139.

[33] Strenkowski, J., Shih, A & Lin, J, "An analytical finite element model for predicting three dimensional tool force and chip flow", *International, Journal of Machine Tool and Manufacturing*, 42, 2002, pp, 67-73.

[34] Ramesh, M. K.N. Seetharamu, N. Ganesan and G. Kuppuswamy, "Finite element modeling of heat transfer analysis in machining of isotropic materials", *International Journal of Heat and Mass Transfer*, 42, 1999, pp 1569–1583.

[35] Mitrofanov, A., Babitsky, V. and V. Silberschmidt, "Finite element simulations of ultrasonically assisted turning", *Computational Materials Science*, 28, 2003, pp 3-4.

[36] Mitrofanov, A., V.Babitsky and V.Silberschmidt, "Finite element modeling of ultrasonically assisted turning of Inconel 718", *Journal of Materials Processing Technology*, 153-154, 2004, pp 233-239.

[37] Mitrofanov, A., N.Ahmed, V. Babitsky and V. Silberschmidt, "Thermomechanical finite element simulations of ultrasonically assisted turning", *Computational Materials Science*, 32, 2005, pp 463-471.

[38] Mitrofanov, A., N.Ahmed, V. Babitsky and V. Silberschmidt, "Effect of lubrication and cutting parameters on ultrasonically assisted turning of Inconel718", *Journal of Materials Processing Technology*, 163, 2005, pp 649-654.

[39] Ahmed, N., A.Mitrofanov, V. Babitsky and V. Silberschmidt, "Analysis of material response to ultrasonic vibration loading in turning Inconel718", *Materials Science and Engineering*, 424, 2006. pp 318-325.

[40] Amini, S., H.Soleimanimehr, M.J.Nategh, A.Abudolah and M.H.Sadeghi, "FEM analysis of ultrasonic vibration-assisted turning and the vibratory tool", *journal of material Processing Technology,*201, 2008, pp.43-47.

[41] Klocke, F.,H. Kratz, "Advanced tool-edge geometry for high-precision hard turning",*CIRP Annals*, 54, 2005; pp 47–50.

[42] Adachi, K., N. Arai, S. Harada, K.Okita and S.Wakisaka, "A study on burr in low frequency vibratory drilling of aluminum", *Surface Metrology, Measurement Science and Technology*, 8, 1997, pp. 955-972

[43] Wu, Y. and Y.Fan, "Develop an ultrasonic elliptical vibration shoe center less technique", *Journal of Materials Processing Technology*, 156, 2004, pp 1780-1787.

[44] Berlh, D.E., and T.A.Dow, "Review of vibration-assisted machining", *Precision Engineering,*32, 2008, pp. 153-172.

[45] Roark, R.J. and W.C. Young, "Formulas for stress and strain", 5th ed., McGraw-Hill, NY, 1975.

[46] ANSYS® 12.0 User guides.

[47] Myers R. and D. Montgomery., "Response Surface Methodology, Process and Product Optimization Using Designed Experiments". Wiley, New York, 1995.

[48] Minitab®15.0 User guides.

APPENDIX A

A.1 SUM OF SQUARES (SS)

SS $_{Total}$ is the total variation in the data. SS $_{Regression}$ is the portion of the variation explained by the model, while SS Error is the portion not explained by the model and is attributed to error. The calculations are:

$$SS_{\text{Re}\,gression} = \sum\left(\hat{y} - y\right)^2$$
$$SS_{Error} = \sum\left(y - \hat{y}\right)^2 \qquad \text{A.1}$$
$$SS_{Total} = SS_{\text{Re}\,gression} + SS_{Error}$$

Where y = observed response, $\hat{y}$ = fitted response, and y = mean response.

Minitab displays the adjusted sum of squares and sequential sum of squares. The adjusted sums of squares do not depend on the order the factors are entered into the model. It is the unique portion of $SS_{Regression}$ explained by a factor, given all other factors in the model, regardless of the order they were entered into the model. The sequential sums of squares depend on the order the terms are entered into the model. It is the unique portion of the sum of squares explained by a term, given any previously entered terms.

A.2 DEGREE OF FREEDOM (DF)

Indicates the number of independent pieces of information involving the response data needed to calculate the sum of squares. The degrees of freedom for each component of the model are:

$$DF_{\text{Re}\,gression} = P - 1$$
$$DF_{Error} = n - P \qquad \text{A.2}$$
$$Total = n - 1$$

Where n = number of observations and p = number of terms in the model.

A.3 MEAN SQUARE (MS)

In an ANOVA, the term Mean Square refers to an estimate of the population variance based on the variability among a given set of measures.

The calculation for the mean square for the model terms is:

$$MS = \frac{AdjSS}{DF} \quad \text{A.3}$$

A.4 F-VALUE

F-value is the measurement of distance between individual distributions. As the F-value goes up, the p-value goes down. F is a test to determine whether the interaction and main effects are significant. The formula for the model terms is:

$$F = \frac{MS}{MS_{Error}} \quad \text{A.4}$$

Larger values of F support rejecting the null hypothesis that there is not a significant effect.

A.5 p-VALUE

p-value is used in hypothesis tests to help you decide whether to reject or fail to reject a null hypothesis. The p-value is the probability of obtaining a test statistic that is at least as extreme as the actual calculated value, if the null hypothesis is true. A commonly used cut-off value for the p-value is 0.05. For example, if the calculated p-value of a test statistic is less than 0.05, you reject the null hypothesis.

A.6 MODEL ADEQUACY CHECK

Before the conclusions from the analysis of variance are adopted, the adequacy of the underlying model should be checked

It is always necessary to

- Examine the fitted model to ensure that it provides an adequate approximation to the true system;
- Verify that none of the least squares regression assumptions are violated. Now we consider several techniques for checking model adequacy.

Before the full model ANOVA, several R^2 are presented. The ordinary R^2 is

$$R^2 = \frac{SS_{\text{Re}gression}}{SS_{Total}} \quad \text{A.5}$$

R^2 (R-sq):

$$R^2 = 1 - \frac{SS_{Error}}{SS_{Total}} \quad \text{A.6}$$

Another presentation of the formula is:

$$R^2 = \frac{SS_{\text{Re}gression}}{SS_{Total}} \quad \text{A.7}$$

R^2 can also be calculated as the Correlation $(Y, \hat{y})^2$

Adjusted R^2 (R-sq Adj):

Adjusted R^2 accounts for the number of factors in your model. The formula is:

$$R^2 = \frac{MS(Error)}{SS_{Total} / DF_{Total}} \quad \text{A.8}$$

BIODATA

BIKASH CHANDRA BEHERA

S/o-Mr.Damodar Behera & Miss. Satyabhama Behera

Correspondence:

Department of Mechanical Engineering,

National Institute of Technology Rourkela,

Rourkela – 769 008, Odisha, India.

Ph: +91 9439782840

E-mail: beherabc@nitrkl.ac.in, bikash.nitr@gmail.com

Web: www.bikashbehera.co.nr

Qualification

Master of Technology (Mechanical Engineering)

NIT Rourkela, [Continuing]

Bachelor of Engineering (Mechanical Engineering)

BPUT (Orissa)

Professional Experience

Project Fellow, NIT Rourkela

Permanent Address:

At-Tentulimal, Po-Aghirapada

Via-Oupada, Dist-Balasore

State-Odisha, India

Pin-756049